Fatigue-Focused Manufacturing Optimization for Welded Structures

by

Carly Mayhood

A dissertation submitted in partial fulfillment
of the requirements for the degree of
Doctor of Philosophy
(Naval Architecture and Marine Engineering)
in The University of Michigan
2021

Doctoral Committee:

Professor Pingsha Dong, Co-Chair
Professor Nickolas Vlahopoulos, Co-Chair
Associate Professor Matthew Collette
Professor Romesh Saigal

Carly Mayhood

mayhoodc@umich.edu

ORCID iD: 0000-0002-2043-3861

ACKNOWLEDGEMENTS

I'd like to thank Dr. Vlahopoulos for his continual guidance and patience through the entirety of this process. Your insights and suggestions were invaluable to me. Thank you to Dr. Dong for sharing your fathomless knowledge on all things welding. Thank you to my committee members, Dr. Collette and Dr. Saigal, for your time and feedback.

Thank you to the other members of the Welded Structures Lab, particularly Shaopin Song, Sandipp Krishnan Ravi, and Xianjun Pei, for exposing me to new research and always acting as my sounding boards.

Thank you to Dr. Sungmin Lee for teaching me so much about the trial and errors of optimization programming and how to work through them.

Thank you to the Joining Team at the Ground Vehicle Systems Center, including Martin McDonnell, Matt Rogers, Dan Wagner, and Demetrios Tzelepis, who provided great technical support and ensured this work remained practical and applicable.

And lastly, thank you to my family, friends, and Chris Kroh for being the best cheering section anyone could ask for.

TABLE OF CONTENTS

LIST OF FIGURES

Figure

LIST OF TABLES

Table

ABSTRACT

Welded structures have an inherent vulnerability of fatigue failure at joint locations due to change in geometry and material properties. The U.S. Army, in an effort to to increase overall readiness, has taken interest in understanding fatigue behavior and failure prevention specific to their ground combat vehicles. Fatigue testing of armor-grade joints was conducted in order to understand the material behavior, and this work incorporates the information developed from these tests with structural load cases to create a proactive assembly plan. By acknowledging the higher stress regions from typical (i.e., high frequency) loading scenarios and avoiding weld placement in these areas, reduced vehicle vulnerability can be achieved.

Current fatigue life optimization research centers around topographical analysis of structural components, primarily focusing on shape and weight with fatigue limits. These optimizations rarely, if ever, consider the manufacturability and cost of the component or structure. This work develops optimization algorithms, tailored to meet manufacturing limitations, with the primary objective of minimizing weld stress exposure and a secondary consideration of cost.

The final algorithm takes direction from bin-packing optimizations by filling in a representative vehicle side panel with a set of designated plate sizes, and evaluating the stress exposure and cost based on the weld placements and weld types. The stress exposure is determined by the position of the weld and scaled by the weld type. The

cost of the assembly considers the overall length of welds and wasted material. The panel assembly designs are then ranked by these evaluations. Results provide a comprehensive, feasible assembly plan that extends the fatigue life of a structure.

CHAPTER I

Introduction

1.1 Motivation

Figure 1.1: Examples of fatigue failure on ground combat vehicles.

The motivation for this work is to increase the readiness of U.S. Army ground combat vehicles by increasing the fatigue life of the structure. While there are continuous improvements in defense and armor technologies to perform and survive in the combat arena, these vehicles still have an underlying vulnerability in fatigue cracking

of the welded joints, which are necessary to assembling the structure, from repeated, low-level loading.

This vulnerability inherent to welds stems from changes in geometry, material characteristics, and residual stress.

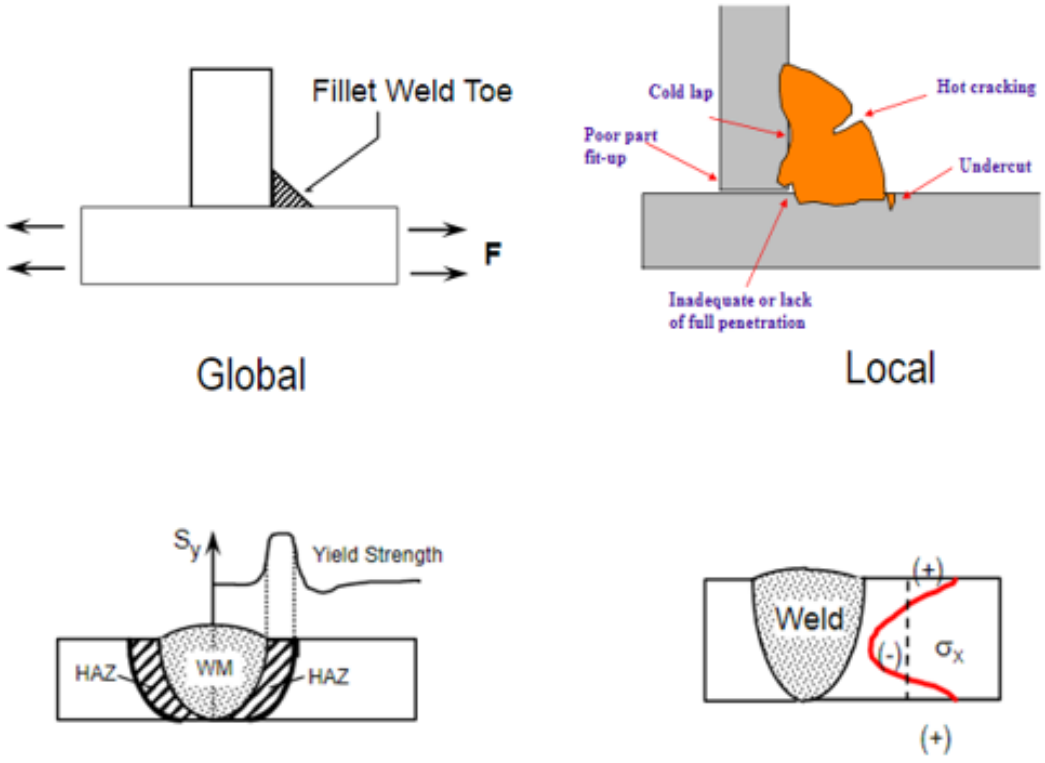

Figure 1.2: Illustrations of geometric discontinuities, weld heterogeneity, and residual stresses (1).

The change in geometry, unavoidable in a weld bringing two components together, acts as a stress concentration point. This means the distribution of stress across the specimen changes at this location and can result in more vulnerability for developing fatigue cracking at this point [1]. The effects can be minimized by insuring proper

alignment of the structural parts being joined through the weld positioning, but not totally excised.

The material characteristics throughout the weld vary between the base metal and the filler material. Often the filler material, or consumable, exhibits a higher yield strength than the base material, but may not always be the case, as is discussed later when looking at armor-grade base materials. Additionally, the weld loses homogeny in the surrounding region due to the extreme change in temperature, creating a heat affected zone (HAZ), leading to phase changes. This includes the creation and inclusion of martensite, a microstructure exhibiting higher hardness. The emergence and amount are highly dependent on the carbon content of the material being used. While harder, the resulting microstructure may also be brittle, leading to a greater risk of cracking [2].

The high heat of the welding process runs the risk of creating hydrogen inclusions from water vaporization. The moisture, present in the consumable, the atmosphere, and even an unclean work surface, diffuses and deposits hydrogen into weld, ultimately resulting in what is known as hydrogen cracking [2]. An unclean work surface with any rust or dirt can also create inclusions and pores within the weld which act as crack initiation sites. These are avoidable problems and have been addressed in best practices defined by the U.S. Army Steel Welding Code [3].

Residual stress from the welding process can result in severe distortions (Figure 1.3). This is caused by the expansion and contraction of the workpiece not being adequately considered. Proper clamping and material pre-treatment can reduce the deformations induced in the process. This is an important consideration because even a slight deformation can cause misalignment or poor fit when the product is fully as-

sembled, which have been shown to have detrimental effects on fatigue performance [4, 5]. This often means refitting and forcing the component into place, which adds new stresses, and the configuration may create unexpected stresses throughout the component, potentially leading to poor performance [6].

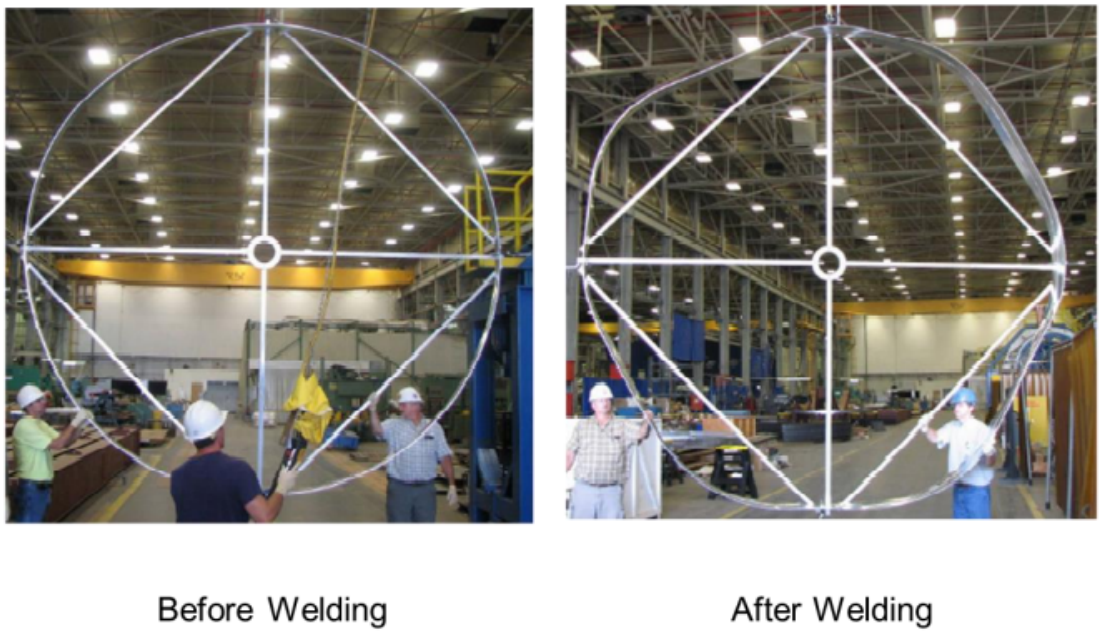

Figure 1.3: Example of distortion from the welding process (6).

This work aims to take these considerations and precautions a step further, by taking into account not only the residual stresses induced from the welding process, but also look at the stress distribution expected during the structure's time. The stress distribution is often analyzed in a finite element analysis program, primarily to ensure safety factor limitations are being met. Since any cyclic stress exposure of a weld decreases the fatigue life of the joint, this work utilizes the information already available from the FEA model to examine ways to improve the life of the structure. If the design of the assembly can avoid weld placement in high stress regions, the fatigue life of the joint extends.

By minimizing the stress exposure of the welds, fatigue failure decreases and therefore the availability of combat vehicles increases.

1.2 Literature Review

Consideration of the fatigue life of a structure has grown with the significant improvements in best practices, materials, and processes. Welders consider the environment, temperature, cleanliness of material, and heat input of the process in order to prevent hydrogen cracking and inclusions, which previously would have dominated the strength and life of a joint [3]. The U.S. Army has made great strides in material development with high-hard steels that can withstand immense impacts and anti-corrosive coatings to prevent immature weathering [7, 8]. Topographical optimization software provides opportunities to lightweight and strengthen structures in precise, deliberate methods [9].

These advances allow for further fine-tuning of structural performance. Specific to fatigue life of welded assemblies, the automotive industry has made impressive improvements in the practices specific to car assembly. Spot welds can be predictively placed to minimize the residual stress incurred during the process. Individual components, such as brackets, have been topographically redesigned to reduce weight and improve fatigue resistance [10]. The weld placement to attach such items has been analyzed to find the precisely best location to extend fatigue life of the joint [11]. Work in these fields is significant and vital to continuous improvement in design [12, 13, 14, 15, 16, 17, 18].

However, often the producibility and manufacturability are overlooked. If a ma-

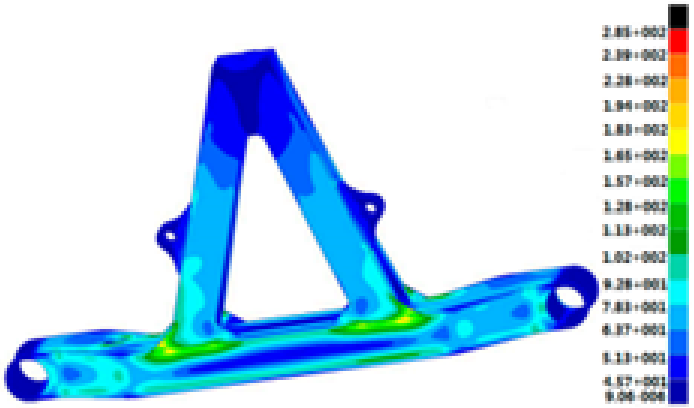

Figure 26. Stress contour of optimized welded A-type frame (MPa).

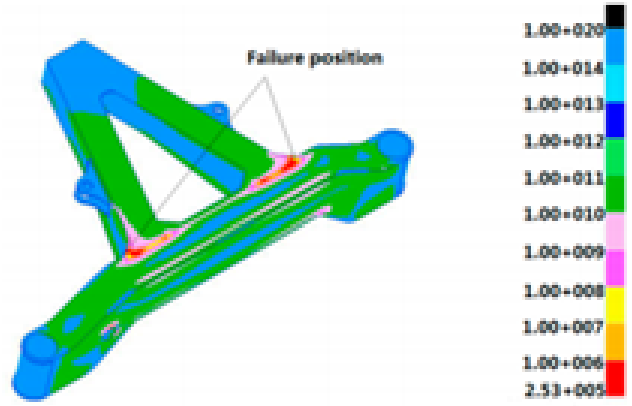

Figure 27. Fatigue life contour of optimized welded A-type frame (cycles).

Figure 1.4: Example of topographical optimization (10).

chinist cannot mill it, or a welder cannot reach it, what is truly the material gain of these improvements? Until additive manufacturing becomes a more viable production method, and automated welding increases in accessibility, the manufacturing setting must be considered.

Additionally, cost is often treated as a by-product of the optimization. If the component is lighter, the design is considered optimized for cost as less material is required. Some works treat material, such as choosing between cast iron and steel, as a variable to meet fatigue criteria and may incorporate an associated material cost

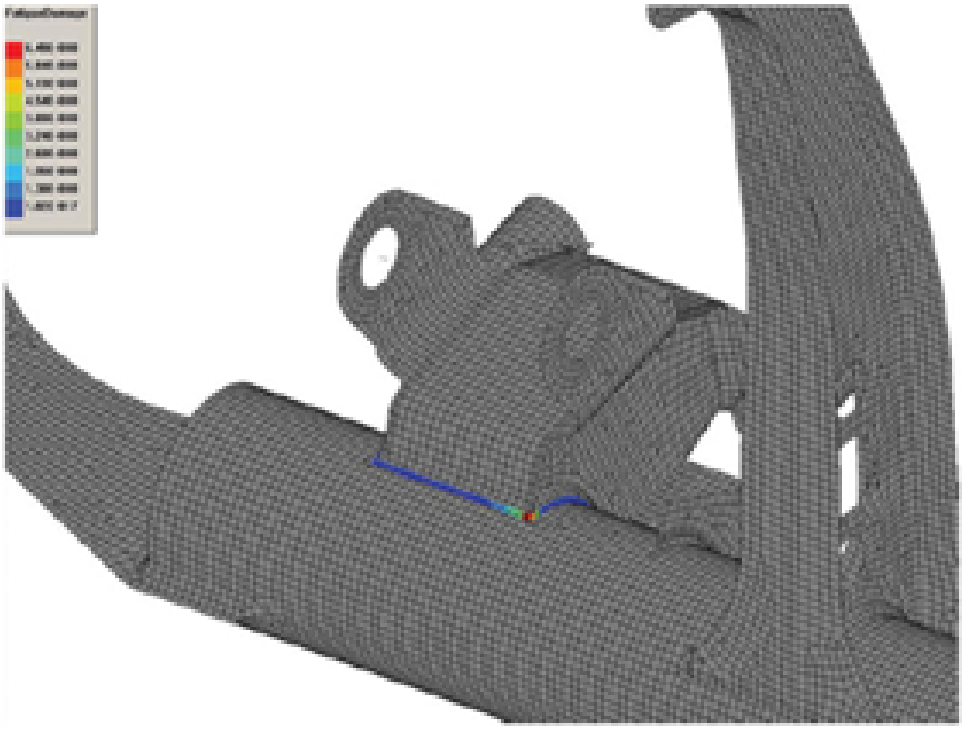

Figure 1.5: Example of weld placement optimization (11).

without considering the significant difference in labor. Largely, a direct change in design to improve fatigue life lacks a comparable analysis of cost.

Manufacturing optimizations have made substantial improvements to the assembly process, albeit typically in very specific conditions [19, 20, 21, 22, 23]. The optimized clamping strategy for a specific part during assembly can greatly reduce distortion. Order of assembly also plays a huge part in distortion reduction and has made great improvements in the functionality of components and structures. However, the design of the actual component or structure does not play a role in these optimizations.

The two bodies of work can be married by restraining design optimization to meet manufacturing limitations and expanding manufacturing optimizations to allow flexibility in the design. This work sets out to make deliberate design decisions within

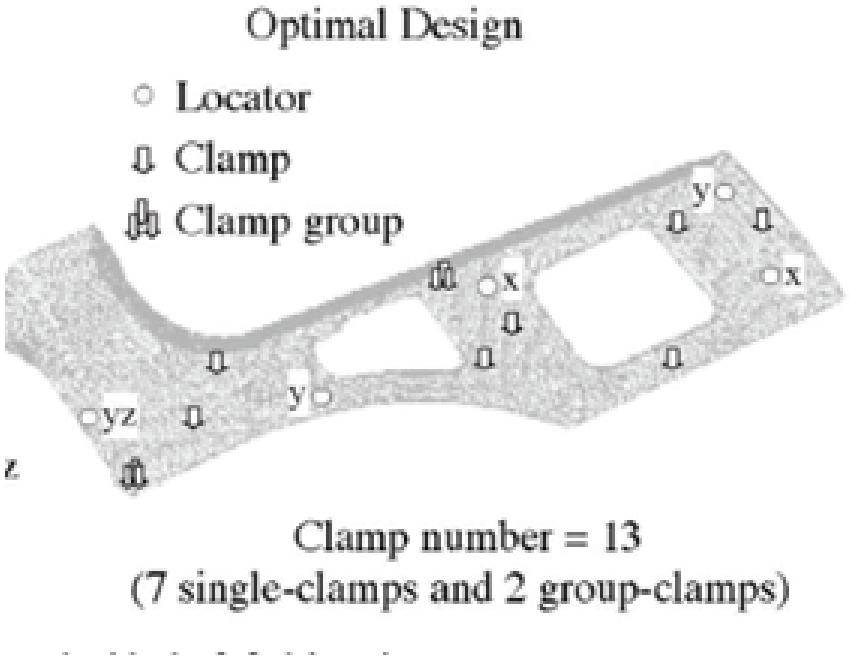

Figure 1.6: Example of clamping optimization (20).

the framework of manufacturability. A structure can be built with tool kits typically seen in bin-packing and sheet cutting scenarios, creating an unique merging of design and manufacturing considerations.

1.3 Method and Approach

This optimization considers changing the assembly of the structure in order to minimize the stress exposure of welds, reducing the risk of fatigue failure. Behavior of armor-grade joints was first analyzed then incorporated into design and assembly of these vehicles through a multi-disciplinary algorithm. The selection of variables include weld type, weld position, and filler material, which all have associated cost implications and stress exposures. The algorithm is unique in that it develops an assembly design which considers both performance (i.e., life of structure) as well as cost within a realistic manufacturing framework.

A representative v-hull structure model was developed in a finite element analysis program, and a stress distribution was generated from a simple loading scenario. This distribution was then referenced by the algorithm for the opening stress exposure at any position on a panel of the structure.

The first development stage of this optimization utilized a genetic algorithm which designated positions of through-width welds on the side panel of the representative v-hull structure. In addition to the position of the weld, the algorithm selected a weld type which scaled the stress exposure based on it's respective stress concentration factor. Lastly, the cost of the assembly was tabulated using the Navy Weld Cost Model, as well as the variance of distance between the welds. Each assembly was evaluated on stress exposure and cost, until the genetic algorithm generated the best case assembly in the final generation.

This work expanded to encapsulate a more realistic manufacturing scenario, where the panel was comprised of several plates, as is common in the assembly of a ground combat vehicle. The addition of horizontal welds meant incorporating a second set of opening stress values. This optimization, dubbed the building block optimization, followed the directional priority set out in work on bin-packing optimizations, commonly used to fill trucks with packages or load ships with containers. Filling in the panel in a way similar to a game of tetris provides a distinctive methodology for assembly design creation. The parameters of the optimization are highly customizable to the restrictions or preferences of a manufacturer or designer. The final development stage of the algorithm covered high stress regions first and promoted similarity within the assembly design. The set of designs were then ranked by Monte Carlo analysis, identifying the top ranked assembly plan based on stress exposure and cost.

This optimization provides a tool kit capable of incorporating performance and cost parameters into design considerations while maintaining and emphasizing the manufacturability of the structure.

CHAPTER II

Panel Assembly Optimization

2.1 Introduction

The first optimization discussed considers a typical v-hull structure, assembled panel by panel. The armor-grade material used on these structures is unique to the military, and it was critical to confirm that these plates behave in predictable ways. Instead of changing the overall geometry of the structure, this optimization changes the design of the weld plan. The optimized assembly considers how the structure functions by running a typical load case and assessing the stress distribution. The new design reduces stress exposure and cost in a balanced fashion.

2.2 Material Behavior

First, the fatigue behavior of materials specific to the combat vehicles needs to be understood in order to incorporate the information into the optimization. The armor-grade materials exhibit uniquely high hardness and had to undergo systematic fatigue testing in order to ensure accurate estimation the fatigue life of these welded joints.

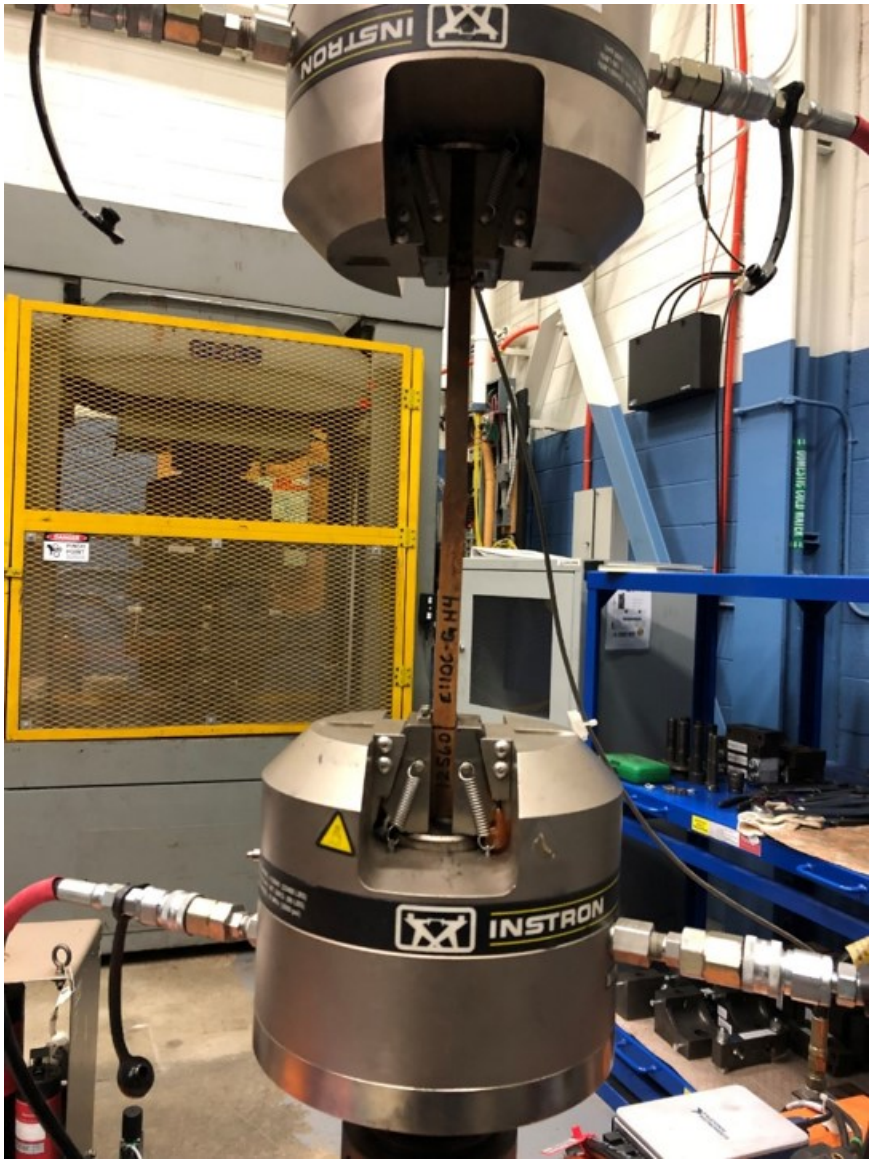

Figure 2.1: Armor Joint in Fatigue Tester.

Multiple combinations of base metals and filler materials are in use on combat vehicles, depending on the build depot and era of build. The mismatch ratio, defined as the yield strength of the consumable over the yield strength of the base metal, was used as the defining characteristic when deciding which joints to test. A comprehensive group of material combinations was selected to fill out a welded joint S-N curve [26], as shown in Figure 2.4. Three combinations were initially tested.

Base Material	Consumable	Mismatch Ratio
MIL-DTL-12560	E110C-G H4	0.665
MIL-DTL-12560	ER70S-6	0.415
MIL-DTL-46100	ER316LSi	0.283

Table 2.1: Tested material combinations and mismatch ratios.

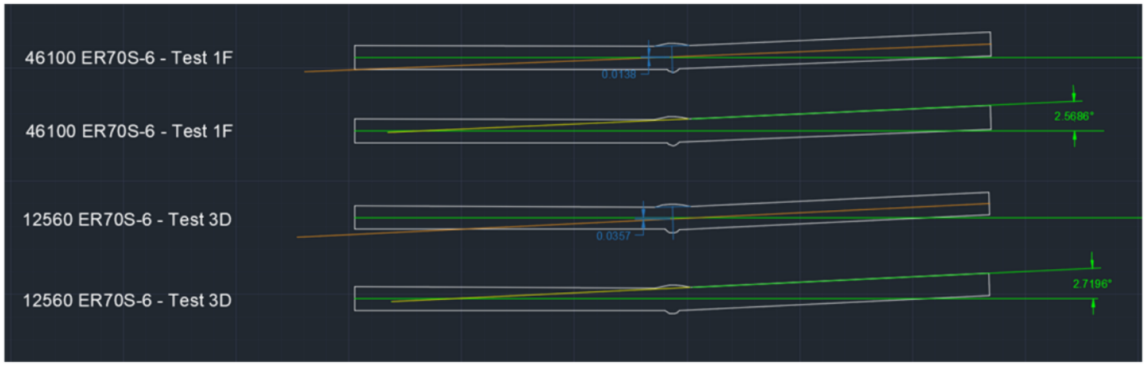

Figure 2.2: Sketches of welded joint samples.

These three combinations represent the highest, lowest, and mid-range mismatch ratios, providing a complete understanding of behavior. Several quarter-inch welded joint strips of each variation were fatigue tested at load cases ranging from 16 to 20 kips.

The last consideration that had to be taken into account for the fatigue life of these samples was the significant angular distortion each joint uniquely exhibited. This distortion, induced from the initial welding process as well as cutting the larger plate into sample strips, varied significantly between material combinations. When the fatigue tester clamped onto these samples, the specimen straightened out, inducing a stress concentration at the weld. This stress needed to be accounted for to develop a more accurate fatigue test.

Therefore, each sample was traced before testing (Figure 2.2), and the tracing was brought into a finite element model (Figure 2.3). The analysis of the model produced

Figure 2.3: FEA model of welded joint for clamping analysis.

a value for the clamping-induced stress which could then be subtracted from the overall fatigue evaluation. The results were plotted onto a Master S-N curve scatter band of welded joints [5, 6].

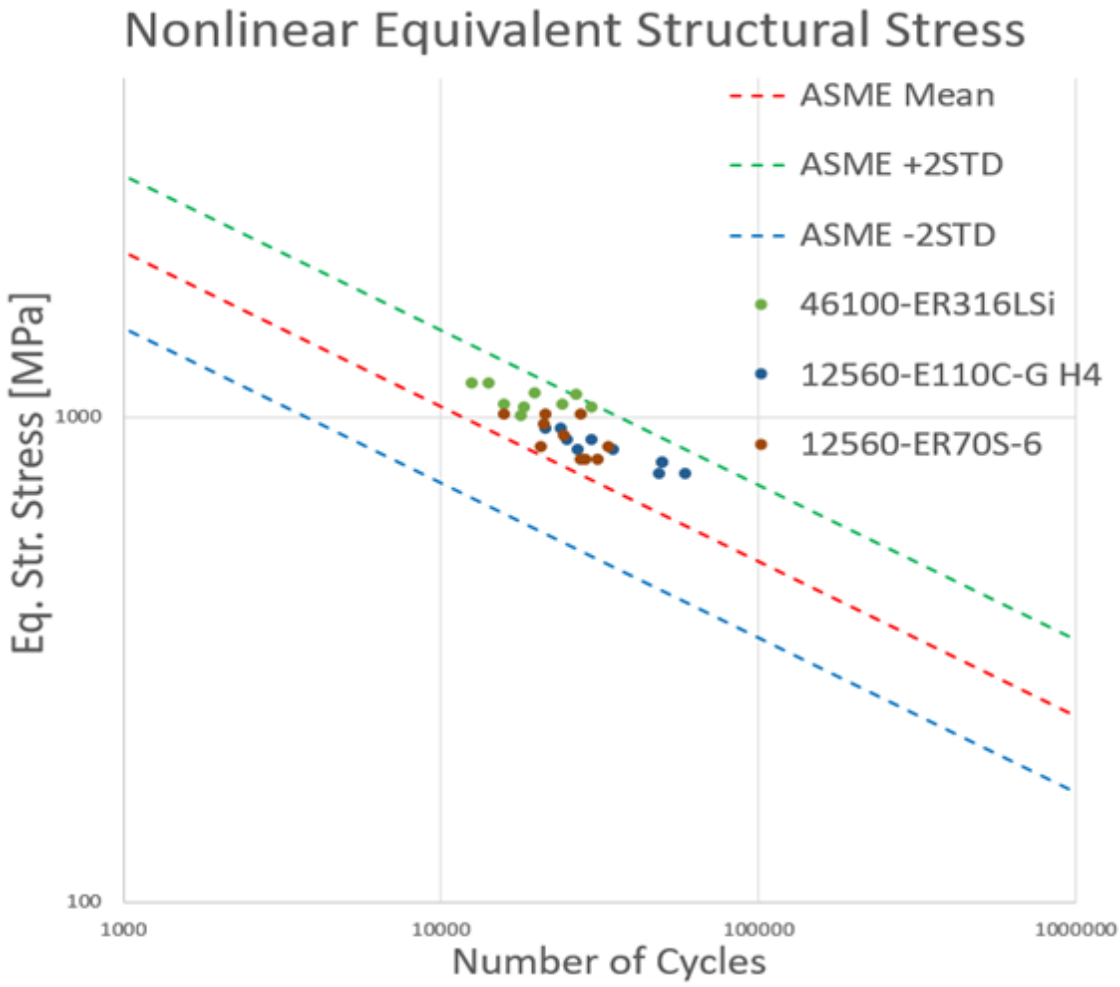

Figure 2.4: Master S-N plot of tested welded joints.

As shown in Figure 2.4, the armor-grade joints fell within the master S-N curve

scatter band defined by mean plus/minus two standard deviations and trend with the mismatch ratios. Therefore, the materials used on the ground combat vehicles behave similarly to standard welded joints, and the optimization can proceed. The algorithms can now utilize the measured fatigue predictability of the welds as an evaluation criteria and ultimately determine the ranking of a design.

2.3 Modeling

A fundamental aspect of this work is an accurate understanding of the loading the structure experiences. The load case used in this optimization should represent the most frequently encountered conditions, since fatigue failure occurs after numerous cycle exposures rather than at a single maximum amplitude. For proof of concept, this work looks at a generic v-hull structure with the finite element analysis software Abaqus [27] under static loading, with reactionary forces acting on all four corners, and a central, downward force representing the weight of the engine.

Because welds are most vulnerable to failure from opening stress, i.e., the stress component perpendicular to weld direction, the optimization considers the σ_x values for the panel running along the length of the vehicle, as shown in Figure 2.6, for through-width welds. These stress values from the finite element analysis are used in the stress calculation during the optimization process. Each panel is individually analyzed for assembly.

The main objective of the optimization is to maximize the fatigue life of the structure. However, the final recommended assembly plan should not add a burdensome price tag, so the cost of the assembly is considered as a second objective in parallel. For the sake of simplicity, each node of the model is considered one foot, making the

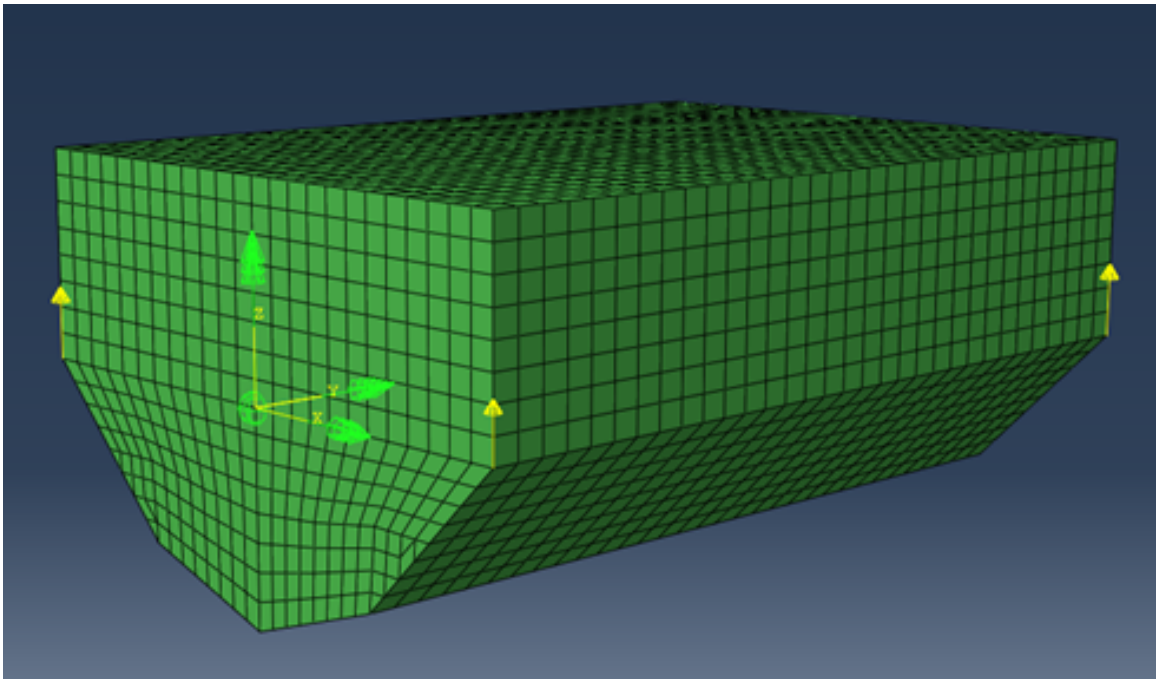

Figure 2.5: Static loads on a generic v-hull structure.

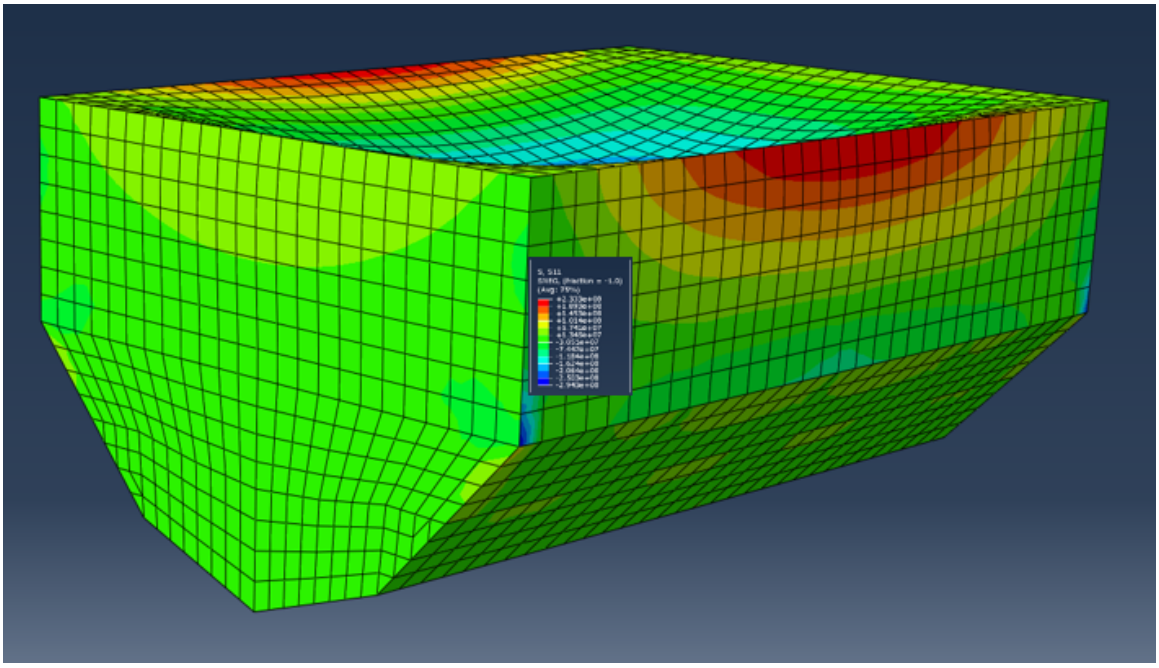

Figure 2.6: Static Load σ_x Values.

length of the vehicle 33 feet, within the range of a typical combat vehicle. Nine-foot plates assemble the 33-foot panel, meaning that the panel requires three welds across its length.

2.4 Optimization Variables

The fatigue life of the structure is measured by the maximum encountered stress for each weld. Just as residual stresses from the welding process can be mitigated by best practices, this optimization works to avoid exposing welds to the stresses of the vehicle 'in-use' by strategically placing the welds outside of high stress areas. Therefore, position is a continuous variable of the optimization.

The filler material of the weld is considered a discrete variable. Since a vehicle is unlikely to be assembled with varying base metals, the two consumables tested with the 12560 base material are used, and their fatigue performance is scaled to the centroid of their distribution along the S-N curve.

The weld type is another discrete variable considered in this optimization, and the selections are flexible to meet the requirements of the design. Three commonly used welds, butt, v, and double-v welds, are the options made available for the assembly. The type of weld scales the maximum stress encountered at the selected position by the stress concentration factor (SCF) specific to each weld designated by the International Institute of Welding [28]. Each SCF is scaled to the lowest performing weld.

Each weld type also has an associated cost based on the Navy's weld cost model [29], which incorporates the labor and material associated with each weld type per unit length. While this model may not accurately determine the actual cost of assem-

bly of a combat vehicle due to the disparity in scale to the Navy, it does provide an accurate comparison of cost between the three weld types, which is the most important factor to the optimization. Again, the three cost factors are scaled to the lowest value.

With all variables (position, weld type, and filler material) defined, the constraints also need to be established. The distance between two welds must not exceed the length of the plate being used to assemble the panel. Additionally, two welds must be no closer than the width of two standard heat affected zones, in order to comply with welding best practices.

2.5 Decision Support Toolkit

Because the optimization needs to consider discrete variables, gradient-based methods are immaterial. Therefore, a genetic algorithm in a mathematical engine decision support toolkit (DST), which can consider discrete variables and multiple objectives, is utilized.

The DST is composed of two parts: a graphical user interface where the user defines the optimization variables, constraints, and flow chart of the optimization as shown in Figure 2.7, and a solver, which runs external applications (in this case, MATLAB [30] executable files) and analyzes and ranks variable combinations.

The optimization considers multiple objectives by evaluating each objective first. Here, stress exposure and cost are the two low-level objectives. Once the algorithm has found the top ranking evaluations for each objective, it feeds these values as reference points into the system level evaluation (SLE), which then balances the distance between the current evaluation and the best-case evaluations as shown in

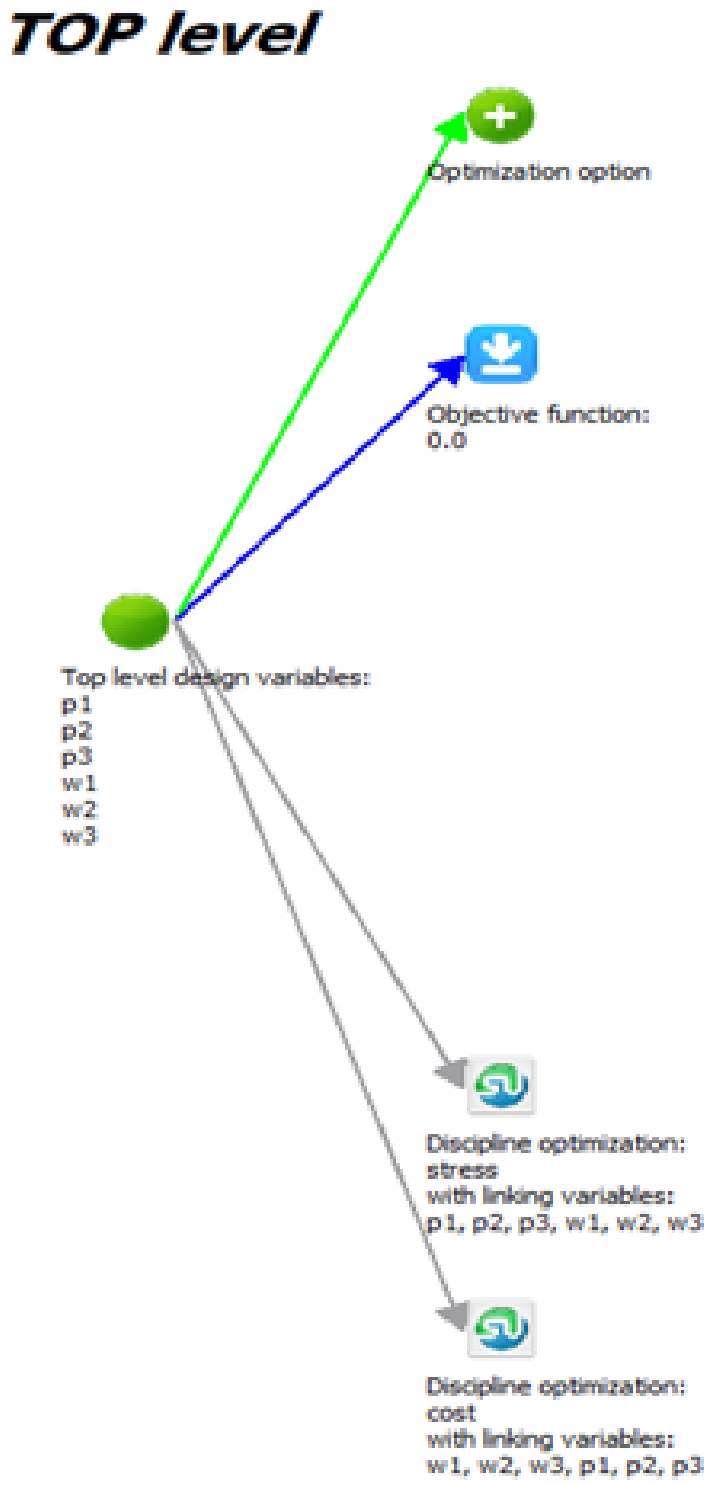

Figure 2.7: Flow chart of the top-level optimization in DST.

Equation 2.1.

$$SLE = min\left(\sum_{i=1}^{N}\left(\frac{Obj^{i,best} - Obj_i}{PRR^i}\right)^2\right) \tag{2.1}$$

The optimization is capable of showing preference for one objective over another by assigning a weight to it; however, in this example, cost and stress exposure are considered equally.

2.6 Multi-Objective Genetic Algorithm

The algorithm generates three welds with associated position, type, and material. The solver passes these variables into the executable files.

2.6.1 Stress Evaluation

The stress evaluation interpolates and pulls the stress encountered (ST) at the designated position of each weld (X) from the finite element analysis, then scales each value by the associated weld type and material (SCF). Lastly, the maximum value of the three stresses (SM) is written into a file which feeds back into the Solver as the evaluation value.

$$for(WeldType)_i$$

$$ST(1, X_i) = ST(1, X_i) \times SCF_i \tag{2.2}$$

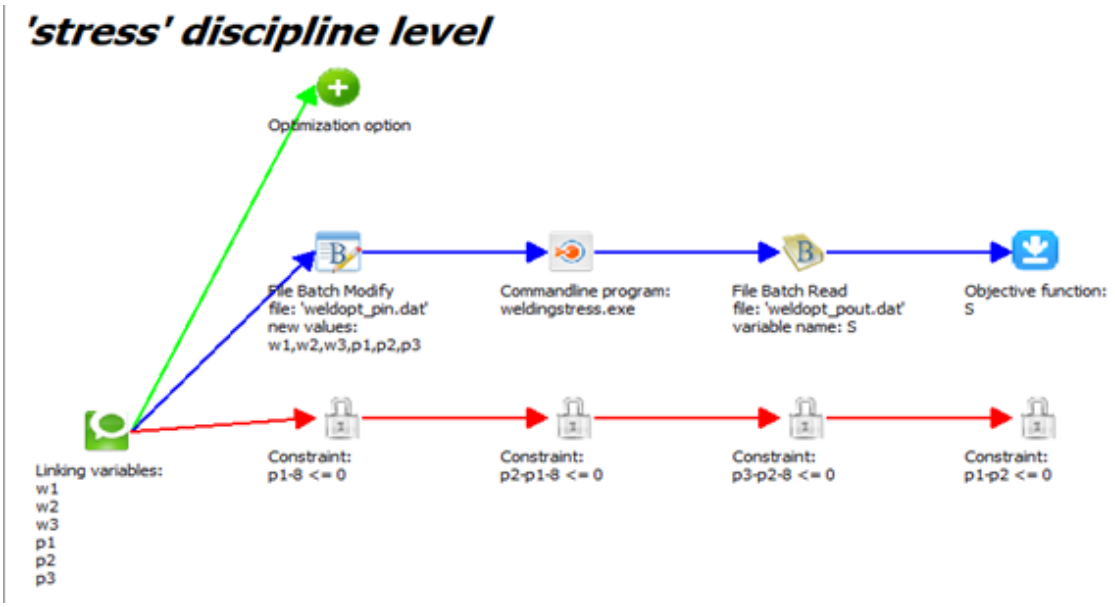

Figure 2.8: Flow chart of the fatigue life level optimization in DST.

$$SM = max(ST(1,:)) \tag{2.3}$$

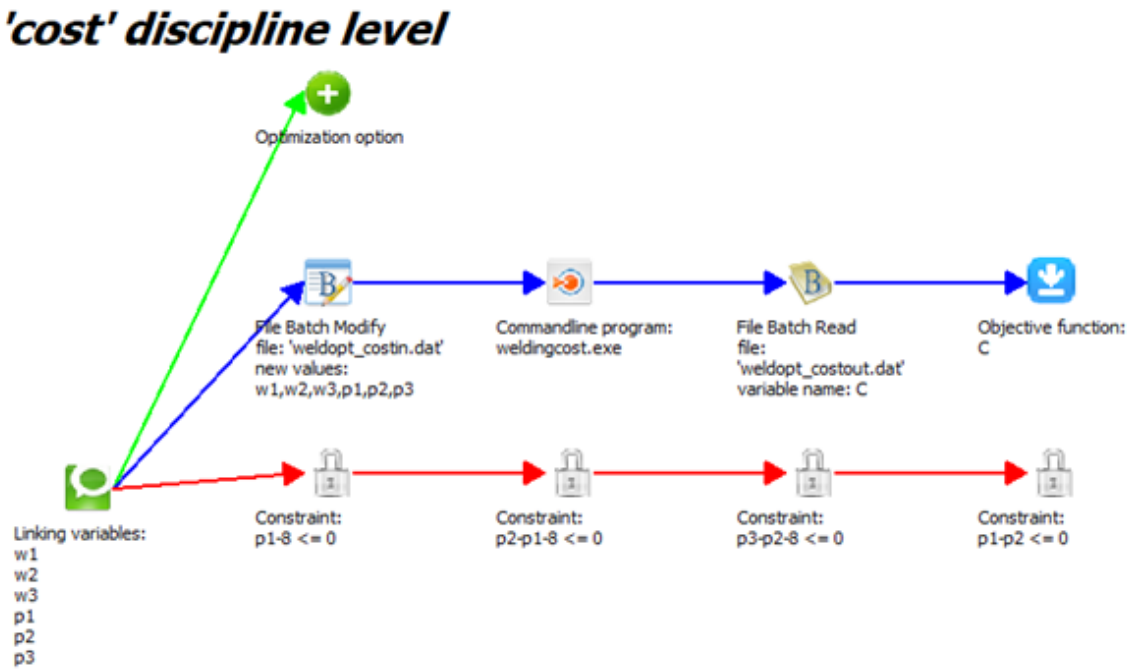

Figure 2.9: Flow chart of the fatigue life level optimization in DST.

2.6.2 Cost Evaluation

The weld cost (C_{wt}) is a measure of the weld type selected since each assembly utilizes the same number and length of welds. Each type has an associated cost factor (wc).

$$for(WeldType)_i$$

$$C_{wt}(1, X_i) = C_{wt}(1, X_i) \times wc_i \tag{2.4}$$

Additionally, the variance of the distance between each set of positions is calculated, under the assumption that a more evenly spaced panel is cheaper. The distance between the edge and the first weld (p_1), the first and the second weld (p_2), the second and third weld (p_3), and the third weld and the edge are defined (SP). Then, the deviance from an evenly spaced assembly (davg=L/4) is calculated into a spacing cost factor (C_{sp}).

$$\begin{aligned} SP = [p_1 - davg)^2, ((p_2 - p_1) - davg)^2, \\ ((p_3 - p_2) - davg)^2, ((33 - p_3) - davg)^2]; \end{aligned} \tag{2.5}$$

$$C_{sp} = sum(SP(1, :))/max(SP) \tag{2.6}$$

The total cost value is calculated by weighted factors of type and spacing. The final cost value is sent back from the executable to the solver in the same manner as the stress evaluation.

$$C_{total} = (C_{sp} \times 0.5) + (C_{wt} \times 0.5); \tag{2.7}$$

The assemblies are ranked by their evaluations. The population and generations numbers (i.e., the number of assemblies evaluated) were increased between runs until a sense of convergence is reached (in this case, when the final generation evaluations were within 10 percent).

The simplicity of these evaluations allowed for individual confirmation of the values. The codes were checked by manually inputting positions and weld types to the input files, having calculated the results externally, and confirming that the results matched.

The decision support toolkit was tested by manually calculating the constraints and validating the values in the results, checking all variables fall within the designated ranges, and confirming that each population had a unique set of variables and evaluations, meaning the generation was not stagnant from improper inputs or outputs.

2.7 Results

The top-ranking fatigue life evaluation sacrifices even spacing to move away from the maximum stress position (at 17 feet) while still meeting the constraints. The stronger weld types are used.

The top-ranking cost evaluation has very even spacing between the three welds and utilizes the cheaper type of welds.

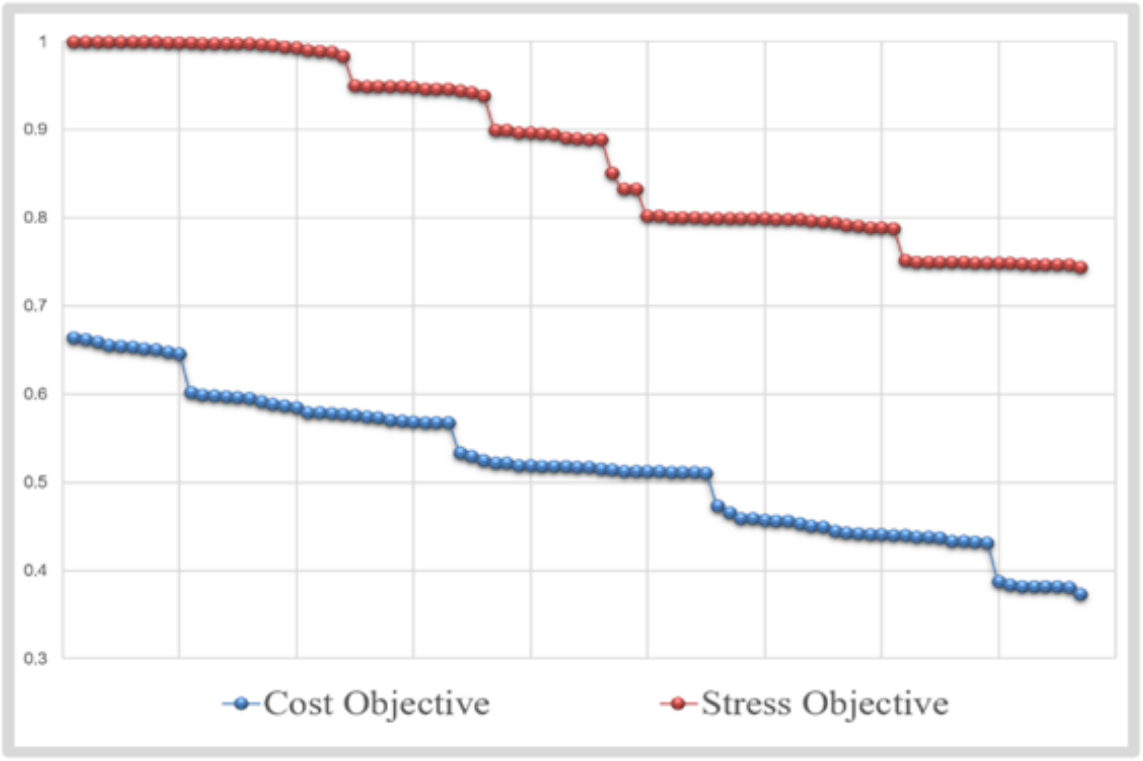

Figure 2.10: Stess and cost evaluations through the GA.

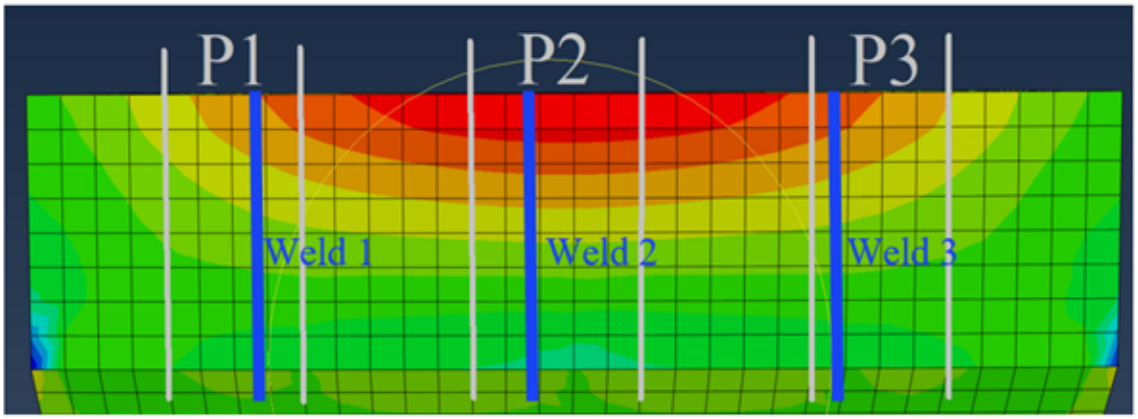

Figure 2.11: The top-ranking fatigue life assembly. Positions 8.89, 15.86, and 24.78, and v, double-v, and double-v welds, respectively.

Finally, the system level evaluation balances the two objectives by only using the strongest, most expensive weld type in the high stress region, and maintains even spacing between the welds.

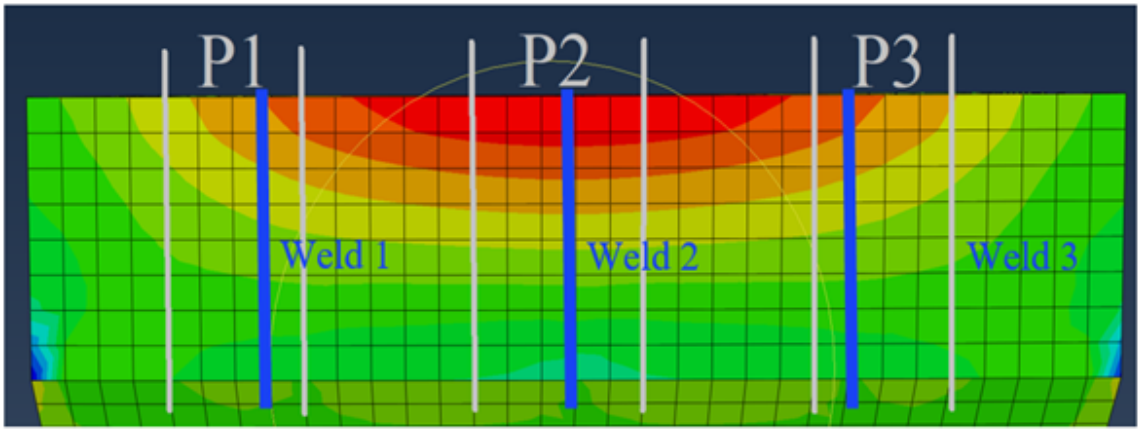

Figure 2.12: The top-ranking cost assembly. Positions 8.16, 16.77, and 24.94, and butt, butt, and v welds, respectively.

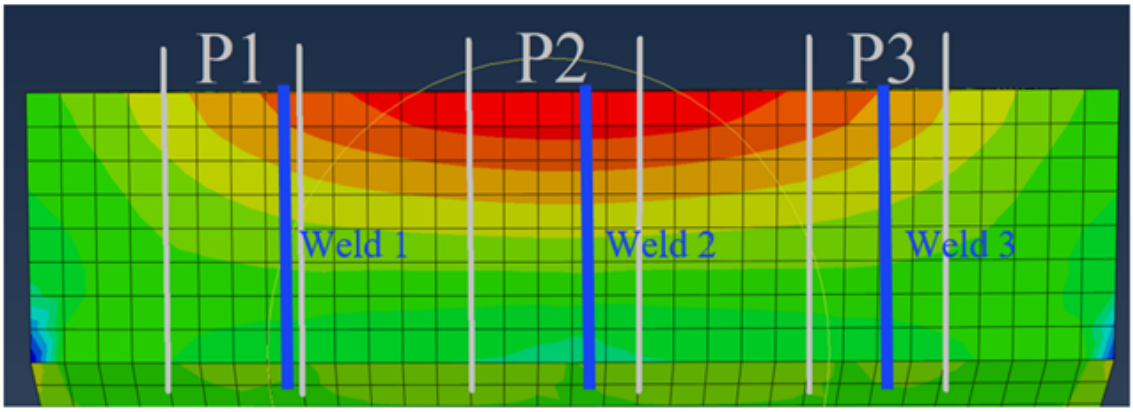

Figure 2.13: The top-ranking system level assembly. Positions 8.78, 17.54, and 26.19, and butt, double-v, and butt welds, respectively.

The optimization proves capability of designing an assembly that minimizes weld stress exposure and therefore maximizing the fatigue life.

2.8 Adding Weld Orientation

The last development stage of this optimization considers adding line orientation to the welds along the panel. Each weld now has an associated angle (a_i) between 30 and 150 degrees in an increment of 10 degrees (30, 40, 50 degrees, etc.). This change in geometry not only allows the weld to avoid areas of high stress, but also changes the magnitude of the opening stress encountered. This requires a stress tensor transformation using σ_x (SX), σ_y (SY), and τ_{xy} (SXY) stress values in order to ensure the evaluation still only considers the opening stress.

if $a_i \leq 90$

$$\begin{aligned} ST(:,j) = SX(:,j) \times (cosd(90 - a(i)))^2 + SY(:,j) \times (sind(90 - a(i)))^2 \\ +2 \times SXY(:,j) \times (cosd(90 - a(i))) \times (sind(90 - a(i))) \end{aligned} \tag{2.8}$$

if $a_i > 90$

$$\begin{aligned} ST(:,j) = SX(:,j) \times (cosd(180 - a(i)))^2 + SY(:,j) \times (sind(180 - a(i)))^2 \\ +2 \times SXY(:,j) \times (cosd(180 - a(i))) \times (sind(180 - a(i))) \end{aligned} \tag{2.9}$$

The cost evaluation adds a penalty proportionally as the angle moves away from 90 degrees to consider the additional labor and potentially wasted material associated with the angles (C_a). Several constraints are added to still ensure no distance between welds exceeds the plate size, and the welds are not allowed to cross over each other.

$$C_a = sum(|90 - a_i|/3) \tag{2.10}$$

The final cost evaluation now has three considerations: weld type, spacing, and angularity. Each factor has a weight assigned by level of importance to the designer

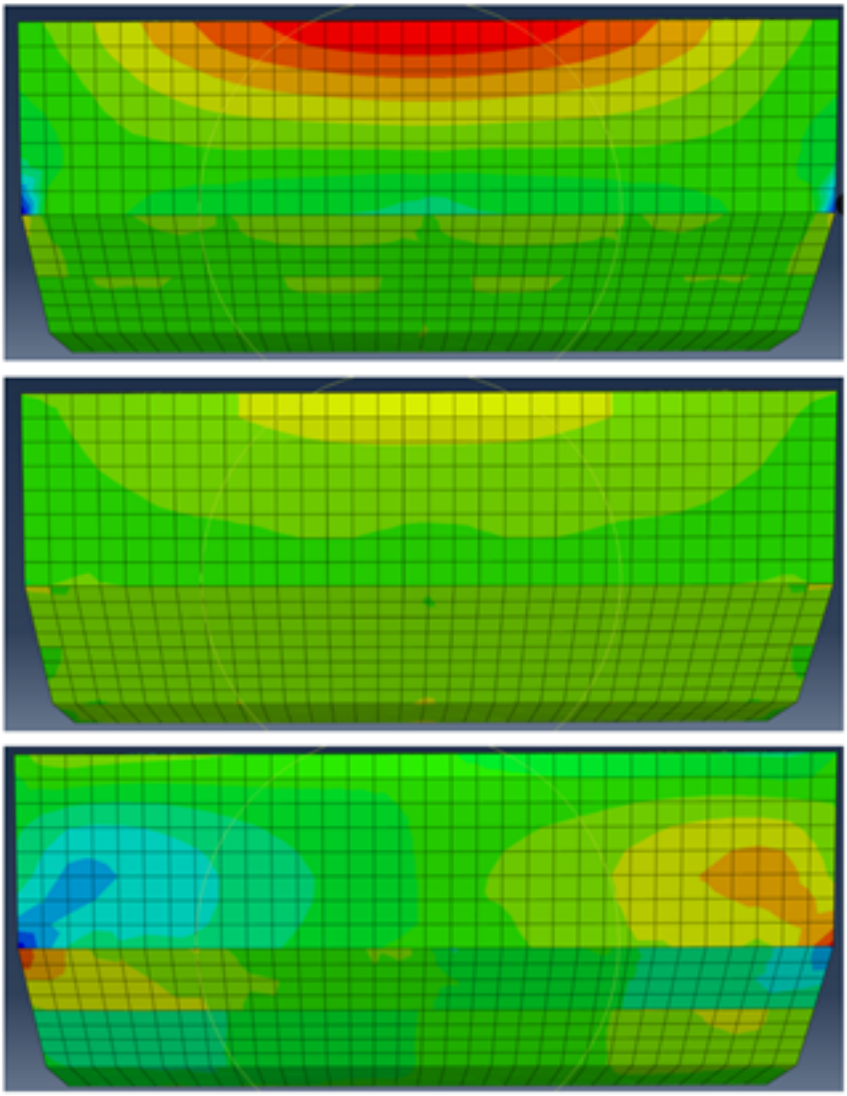

Figure 2.14: σ_x, σ_y, and τ_{xy} stress values used in the transform.

or manufacturer. In this example, the spacing and angularity costs are considered at 20 percent and the weld type at 60 percent.

$$C_{total} = (C_{sp} \times 0.2) + (Ca \times 0.2) + (C_{wt} \times 0.6) \tag{2.11}$$

The additional three variables to each evaluation required an increase in population and generation sizes to reach a sense of convergence.

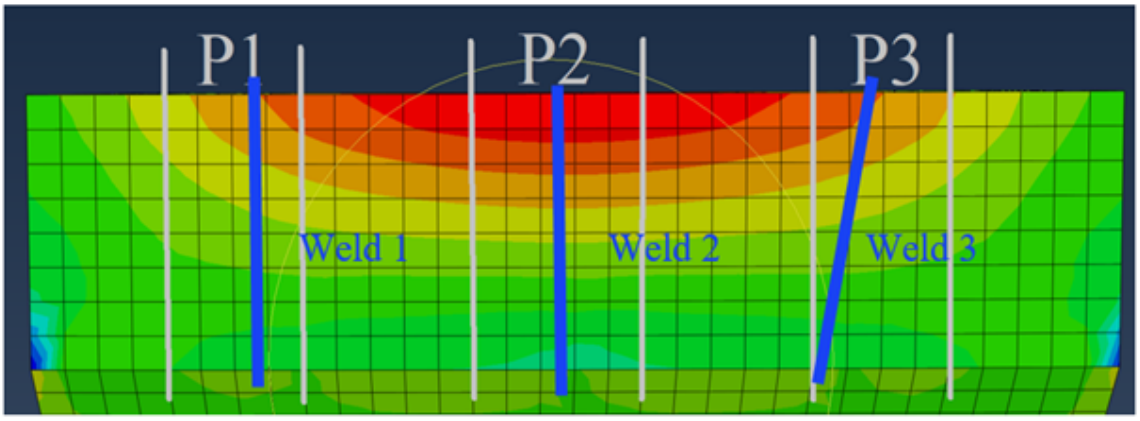

Figure 2.15: The top-ranking system level evaluation including angularity. Positions 7.85, 16.80, 24.02, and butt, double-v, and butt welds, respectively.

While the constraints significantly limit the angularity of the welds, the final result still shows proof of concept. The third weld angles out away from the higher stress. The first weld would violate the constraint if angled away from the stress. The final assembly still indicates the stronger weld type for the high stress region and maintains relatively even spacing.

Panel Assembly Optimization

Stress Evaluation

Step 1:
Open input file from DST, defining weld positions and types.

Step 2:
Pull maximum stress values for the designated positions. Scale by designated weld type SCF.

Step 3:
Output maximum stress value.

Cost Evaluation

Step 1:
Open input file from DST, defining weld positions and types.

Step 2:
Calculate weld cost based on type.

Step 3:
Calculate total cost of welds and scale by most expensive possibility.

Step 4:
Calculate cost associated with spacing (SP). Space defined as SP (p1, p2-p1, p3-p2, 33-p3). Scale by maximum spacing value.

Step 5:
Calculate total cost evaluation by assigning weight to weld type and spacing.

Step 6:
Output total cost evaluation.

Adding Angularity

Step 1:
Calculate the x-distance added or subtracted from angle.

Step 2:
Tabulate the new positions the weld passes through.

Step 3:
Calculate the opening stress with tensor transformation.

Step 4:
Follow Steps 2-3 in the panel stress evaluation.

Overall Evaluation

Step 1:
Calculate overall evaluation value based on designated weight for stress exposure and cost evaluations.

Step 2:
Rank all assemblies. Lowest total evaluation is the highest-ranking assembly.

Figure 2.16: Panel Assembly Optimization Steps.

CHAPTER III

Building Block Algorithm

3.1 Introduction

The panel assembly optimization shows a simplified version of a structure assembly. A typical manufacturing floor may have a few to several sizes of plates available to construct the structure. These plates may not reach the full length and width of the assembly, therefore multiple plates are required with horizontal and vertical welds. This optimization treats these plates as 'building blocks' used to fill out the panel assembly. Maximum fatigue life and minimal cost are still the optimization goals.

3.2 Bin Packing Optimization

This optimization takes its lead from work done to optimize bin packing, seen when filling trucks, ships, and planes [31, 32, 33]. It is also a similar concept to the popular game Tetris, which has seen numerous attempts for an algorithmic solution [34, 35].

The work done in this field has different priorities than the assembly optimization.

For instance, the blocks or packages must not overlap, as such a configuration would be physically impossible. The order of the placement may be an important consideration for unloading the container. The center of gravity of the final configuration may be important to the stability of the transport or the order of packing may need to consider fragile items.

This assembly optimization does not consider order, and it does not prevent blocks from overlapping or even overhanging from the panel. These are circumstances that can be dealt with in the manufacturing setting. However, the guiding principle in bin packing of setting a directional priority was crucial to the success of this optimization. Figure 3.1 shows a bin packing problem with a bottom-left direction. This means the block being placed finds the lowest, left-most position it can occupy.

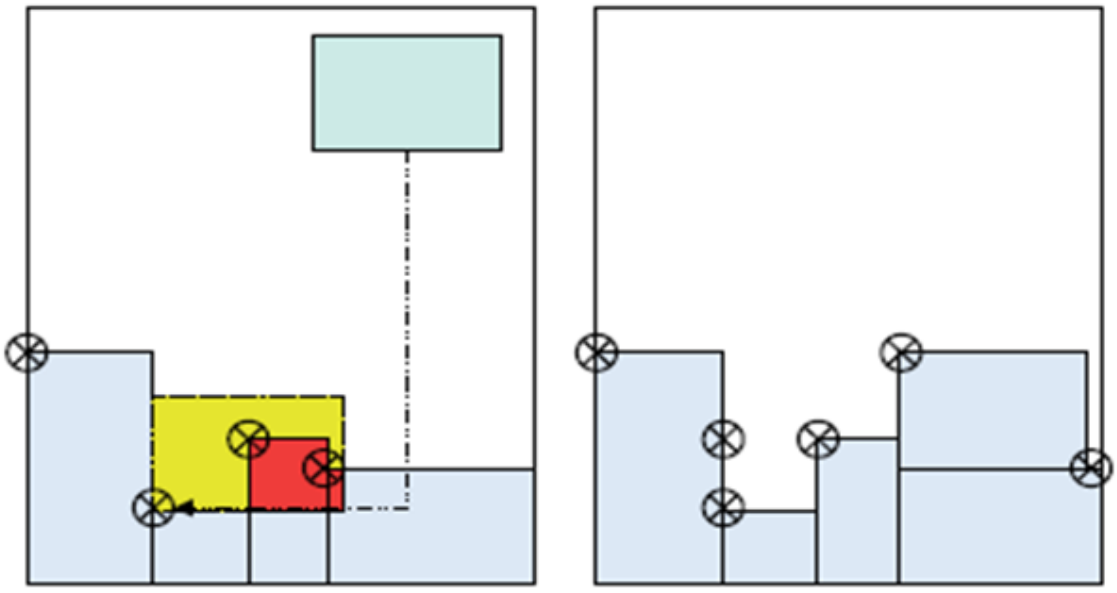

Figure 3.1: Example of directional priority in a bin packing optimization (31).

3.2.1 Modeling

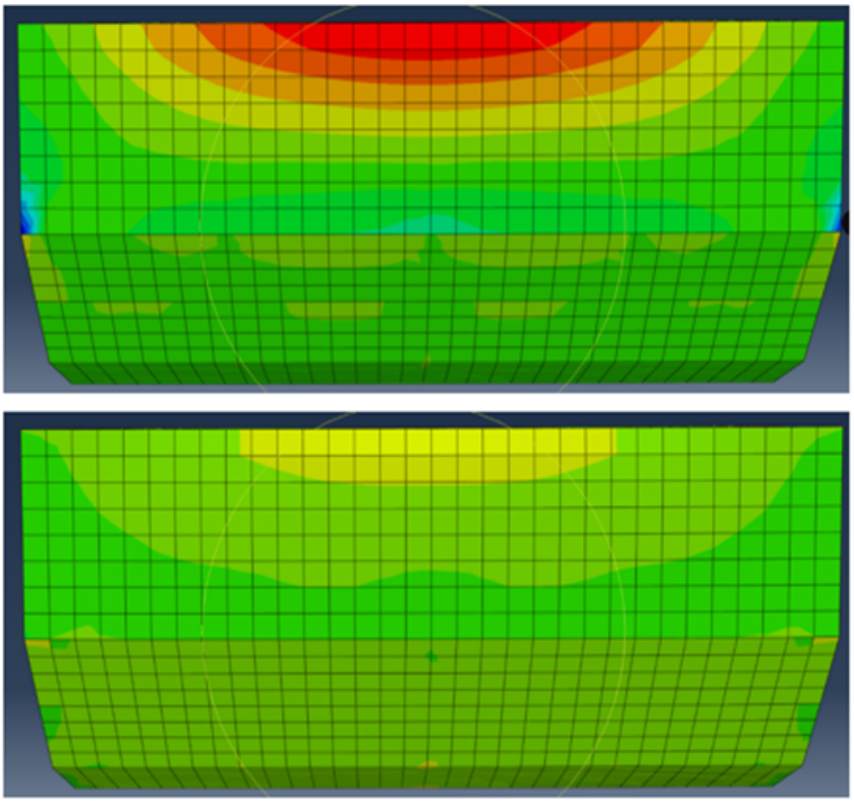

Figure 3.2: σ_x and σ_y values.

Just as the previously discussed optimization required a load case, this optimization also relies on an understanding of stress distribution. The efficacy of the assembly on fatigue life is highly dependent on an accurate load case.

Because this assembly consists of several individual plates, both vertical and horizontal welds are required to fully fabricate the panel. Therefore, values for the opening stress in each direction, that is, in the x- and y- directions, are used to determine the stress exposure for each weld (Figure 3.2). No tensor transformation is required as the welds do not have any angularity. For the sake of simplicity, the same load case as shown previously is used for this optimization. The model values are scaled to meet the dimensions used in this example, and the stress values are interpolated

to the designated positions.

3.2.2 Variables

Vertical Length	Horizontal Length	Roulette Wheel Range
8	4	0 - 0.166
12	4	0.167-0.333
12	5	0.334-0.5
4	8	0.501-0.667
4	12	0.668-0.834
5	12	0.835-1

Table 3.1: Roulette Wheel Ranges for plates in both orientations.

The various plate sizes and orientations are the only variables used in this optimization. In this example, six possible selections as shown in Figure 3.3 from the three plate sizes (8'x4', 12'x4', 12'x5') in two orientations (vertical and horizontal) have equal probability in a roulette wheel selection. Each plate occupies a range: 0-0.166, 0.167-0.333, 0.334-0.5, 0.501-0.667, 0.668-0.834, and 0.835-1. The code randomly generates a value between 0 and 1, and the plate occupying the range in which the value falls is selected for the panel assembly.

3.2.3 Methodology

The optimization begins with an array of zeros representing the panel (P) in length (L) and width (W).

$$P = zeros(W, L)$$

As seen in the bin packing optimization, this work defines a prioritized direction; in this case, to the left and up. This means the program searches for the left-most,

Figure 3.3: Roulette wheel selection of plates.

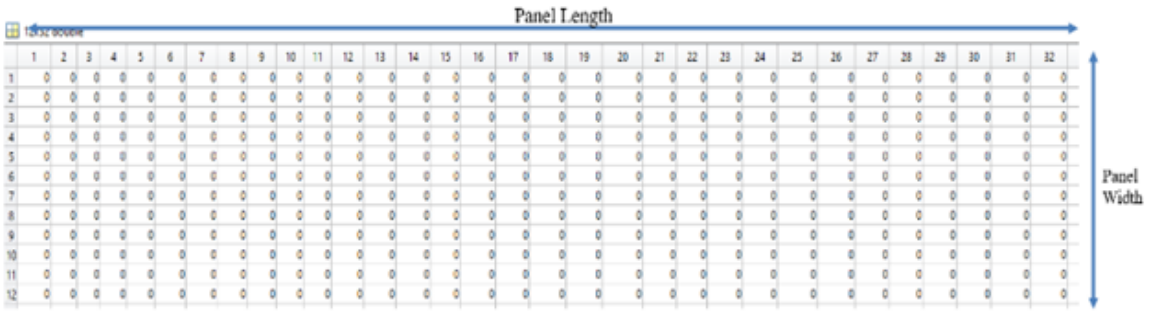

Figure 3.4: A representative panel as an array of zeroes.

top-most unoccupied space of the panel by row (r) and column (c).

$$[r(i), c(i)] = find(P == 0, 1)$$

The next plate of specified dimensions (dim), generated by the roulette wheel, is placed in this position. The zeros in the panel are revised to ones as the space is filled in with a new plate until the entire panel is transformed.

$$P(r(i) : r(i) + dim(1) - 1, c(i) : c(i) + dim(2) - 1) = ones$$

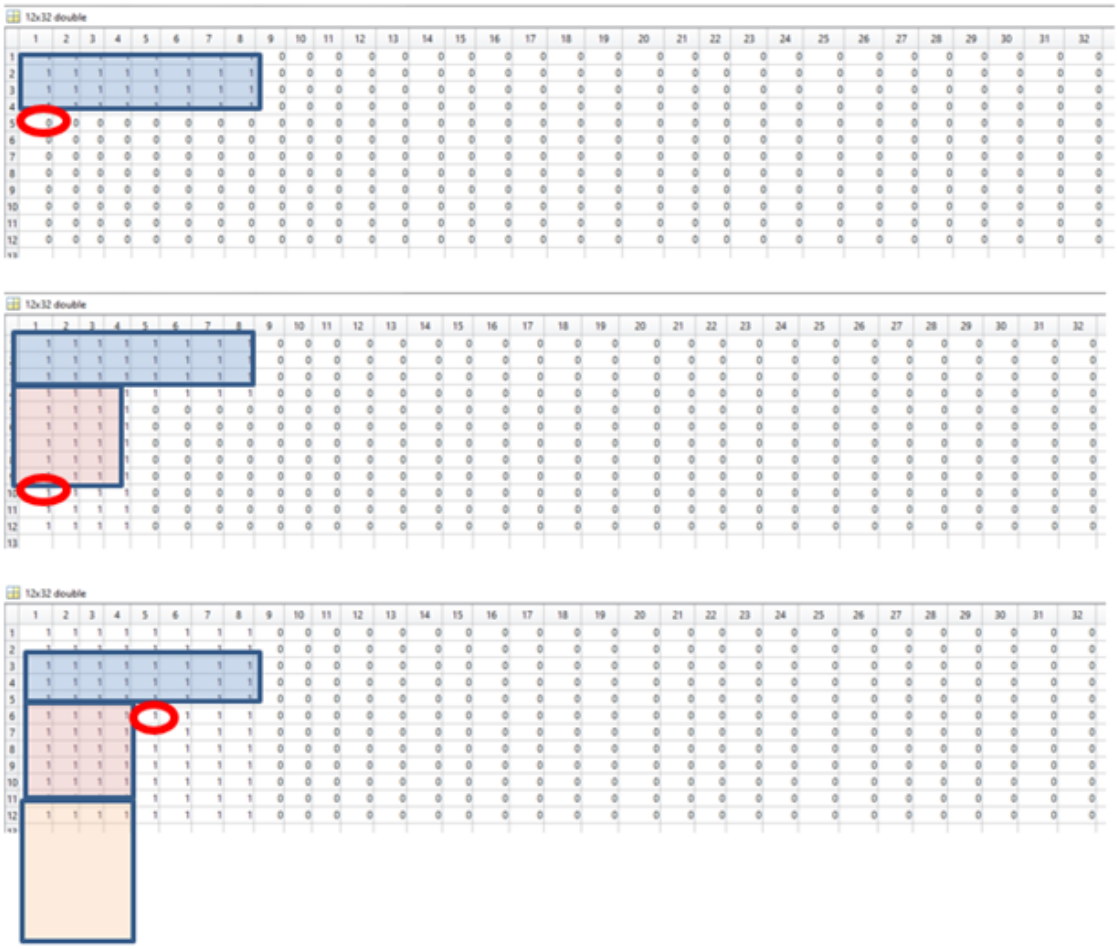

Figure 3.5: Progression of the panel being filled.

As seen in Figure 3.6, the assembly stage of the program allows for overlap and overhang of the plates. The tally of plates for each assembly provides a square footage of the material used (PB). The area of the panel (P) is subtracted from this value to define the material wasted (WM), which is considered in the cost.

$$WM = PB–P \tag{3.1}$$

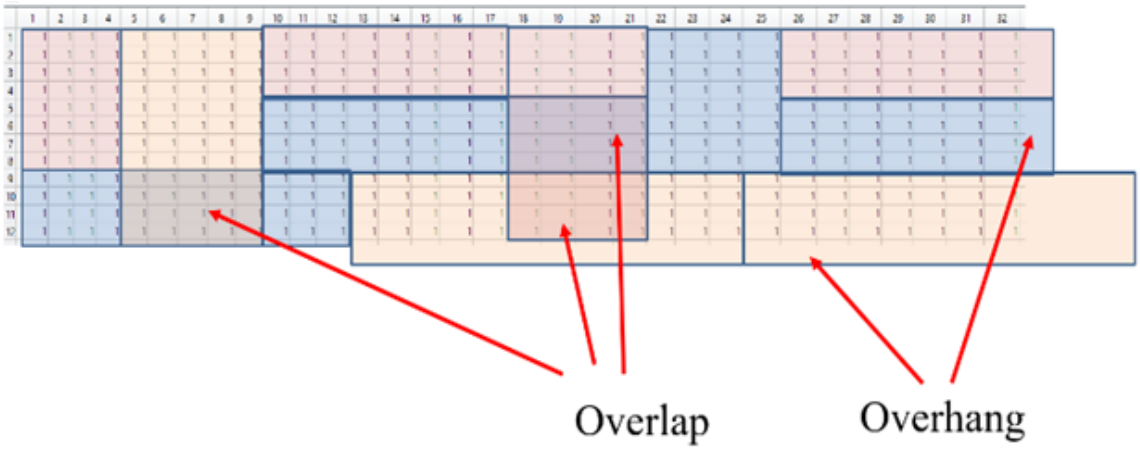

Figure 3.6: The filled panel allows for overlap and overhang of the plates.

At this point, the plates are truncated to the panel borders, and the overlaps are erased with priority given to the earlier plate (i.e., the plate that was placed later in the assembly is 'cut'). Now the vertical (vw) and horizontal (hw) weld positions can be defined by the borders of the plates remaining.

$$vw(i,:) = (c_i, r_i, r_i + w_i)$$

$$vw(i+1,:) = (c_i, +l_i, r_i, r_i + w_i)$$

$$hw(i,:) = (r_i, c_i, c_i + l_i)$$

$$hw(i+1,:) = (r_i + w_i, c_i, c_i + l_i)$$

The total length of welds (TWL) provides another cost point.

$$TWL = sum(hw(:,2) - hw(:,3)) + sum(vw(:,2) - vw(:,3)) \tag{3.2}$$

The vertical and horizontal positions are tabulated separately, as the two sets pull from either the x- or y- opening stress values. Then, the maximum stress encountered produces the value associated with the fatigue life of the assembly.

It should be noted that the average stress encountered over the total length of the welds was initially calculated as well. However, the difference in value was so unappreciable between assemblies that the value was dropped as a factor. This could be revisited in other cases with a more complex stress distribution.

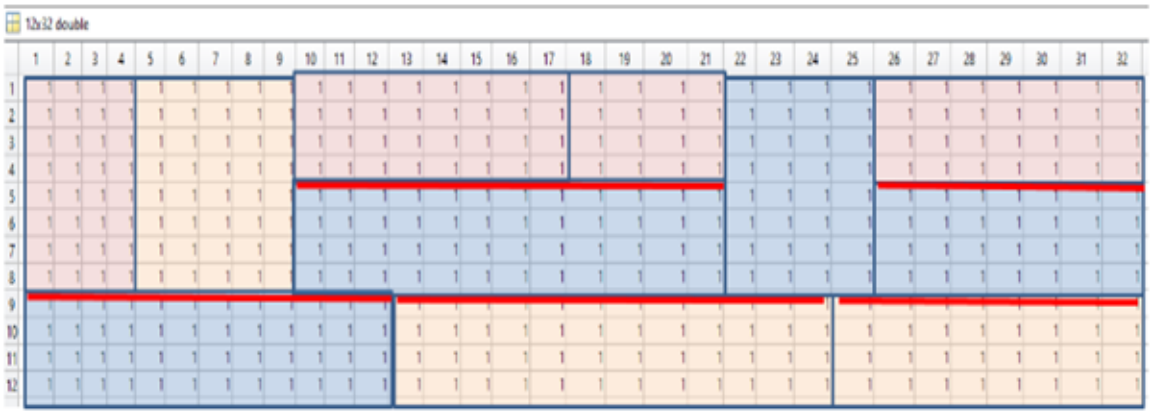

Figure 3.7: Horizontal weld positions.

This process is repeated to create a designated number of assemblies, which will become individual populations within the genetic algorithm. Three factors define each assembly: the material wasted (WM), the total weld length (TWL), and the maximum stress encountered (S). Each factor is scaled to the highest value within the populations, resulting in all values ranging from 0 to 1. The two cost factors, waste and weld length, are averaged together to provide one final cost value (TC). The final assembly evaluation (AE) factors the total cost value and stress encountered.

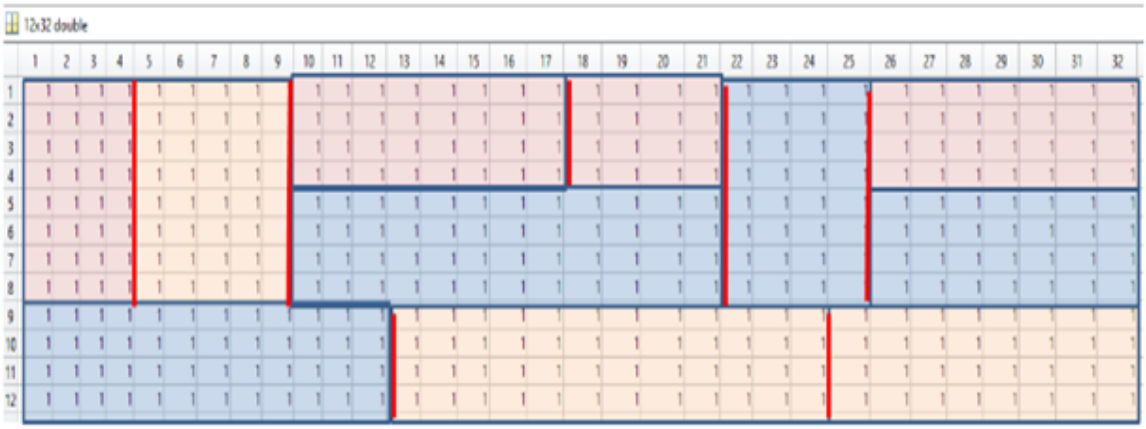

Figure 3.8: Vertical weld positions.

$$TWL_i = TWL_i/max(TWL) \tag{3.3}$$

$$WM_i = WM_i/max(WM) \tag{3.4}$$

$$TC_i = 0.5(TWL_i) + 0.5(WM_i) \tag{3.5}$$

$$S_i = S_i/max(S) \tag{3.6}$$

$$AE_i = 0.5(TC_i) + 0.5(S_i); \tag{3.7}$$

These factors can easily be weighed to assign preference to one over another, depending on the priority of the manufacturer, and the same principle can be applied to the overall cost factor and fatigue life factor for each assembly. In this case, the cost and fatigue life are weighed equally. The set of assemblies is then ranked by the final calculated value. The progression through the rankings shows the assemblies move from wasteful to efficient, from high stress regions to low.

Once again, codes were checked and confirmed by manually calculating values and checking the script produced the same results.

Another code was written to produce visual results of the panel, creating a short video showing how the panel was filled in. This provided an efficient way to check that every design was being completed (i.e., no gaps on the panel) and that the designated directional priority was being followed.

3.2.4 Results

The following results are from a run with 200 generations consisting of 100 populations. This number of assemblies presented a sense of convergence, as the final generation evaluations fell within ten percent of each other.

Figure 3.9: Lowest ranking design.

The lowest ranking design (Figure 3.9) has excessive overhanging plates and incongruous overlapping. This leads to a large amount of wasted material, odd geometries, and significant weld length.

The highest ranking design (Figure 3.10) fits plates neatly together with little

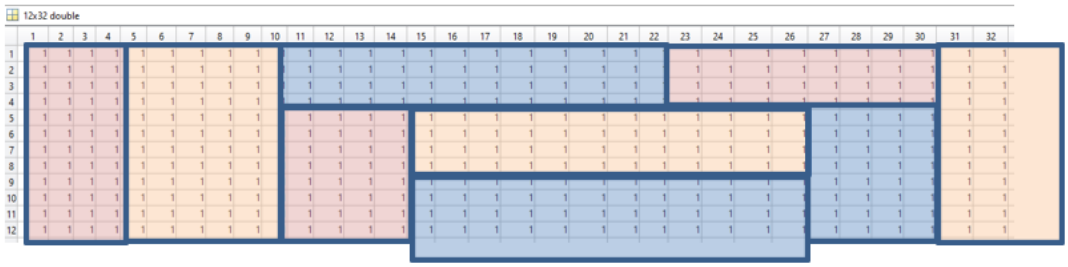

Figure 3.10: Highest ranking design.

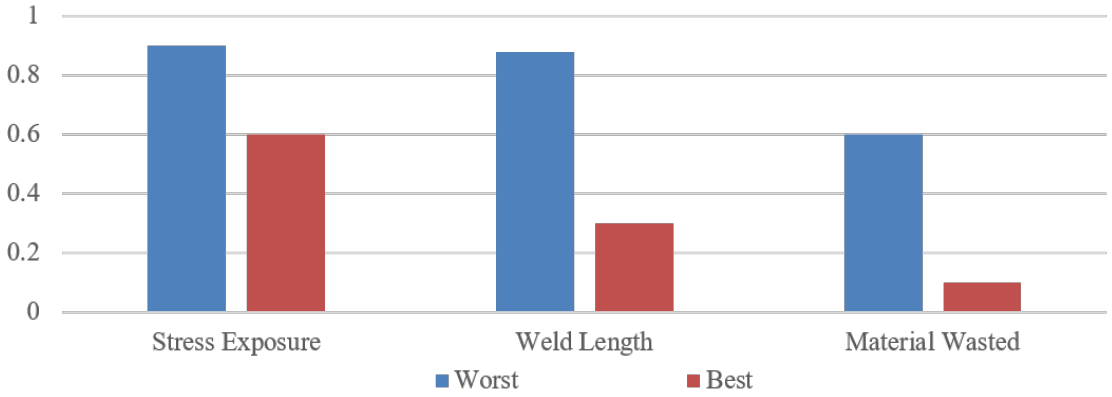

Figure 3.11: Comparison of values for highest and lowest ranking assembly designs.

overhang and no overlap. The lower number of plates used leads to less welds, not only decreasing cost but also vulnerability.

This optimization demonstrates a proof of concept for a building block assembly. The results show a clear, decisive ranking of assembly designs based on cost and fatigue life evaluations.

CHAPTER IV

Plate Considerations

4.1 Introduction

Now that the viability of the building block algorithm has been proven, additional considerations are added to improve the manufacturability and performance of the design. This primarily focuses on the plates, or building blocks, of the optimization.

4.2 Rolling Direction

In the first development stage of the algorithm, the plate selections included both the vertical and horizontal orientations. This doubled the number of options in the roulette wheel (i.e., three plate sizes led to six selections), creating a wide variety of assembly designs. However, the rolling direction from the plate production can significantly affect the performance of the metal plates and must be considered in the build.

The rolling direction is a product of the extrusion process when a metal plate passes through rollers to reduce thickness. The initial, thicker slab of metal commonly has inclusions or porosity imperfections from the manufacturing process. These defects act as stress concentration points and are more prone to cracking and failure.

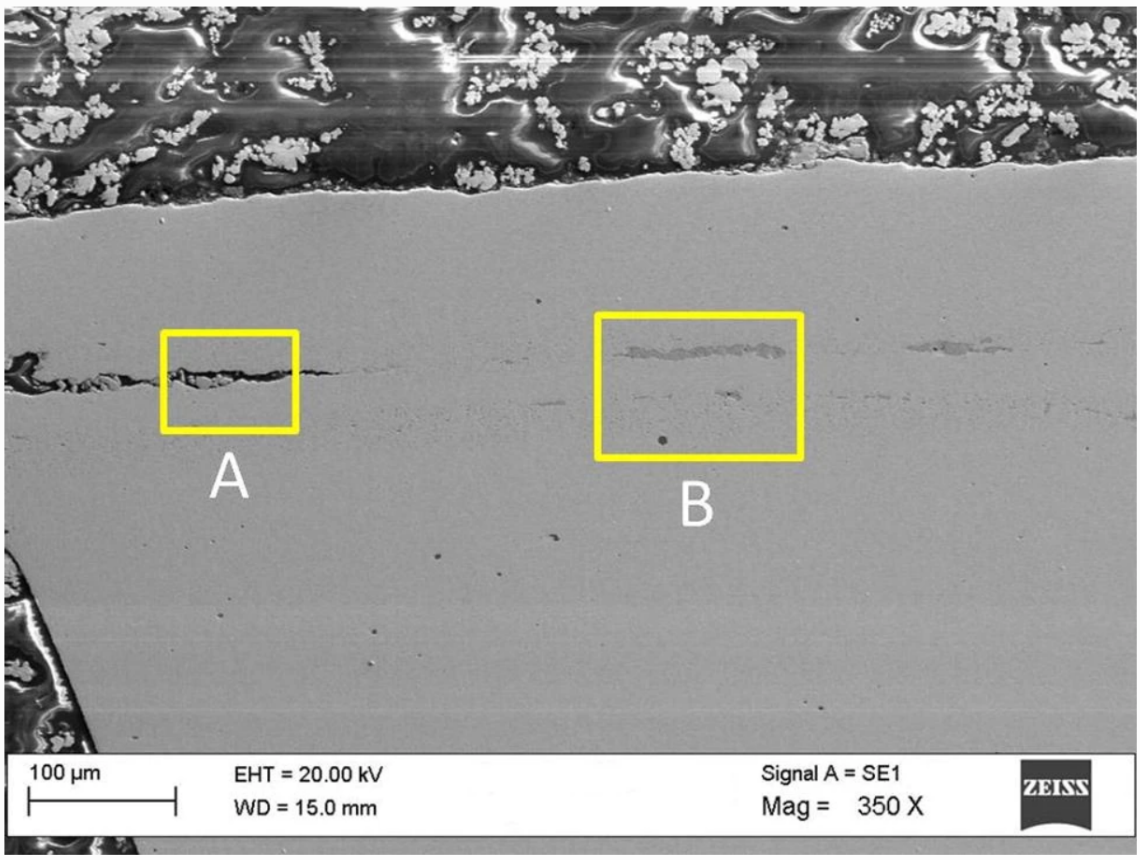

Figure 4.1: Example of elongated defects in a rolled sample (36).

When this material moves through the extrusion process, these pores or inclusions elongate in the rolling direction. These defects now have a significantly larger surface area perpendicular to the rolling direction. The discrepancy of surface area in the x- and y- directions creates a vulnerability in one direction, as any stress or bending encounters nearly no defect in one direction and a sizable defect in the other.
Because of this vulnerability, the plates now are only considered in the horizontal orientation, consistent with the rolling direction, in the algorithm [36, 37].

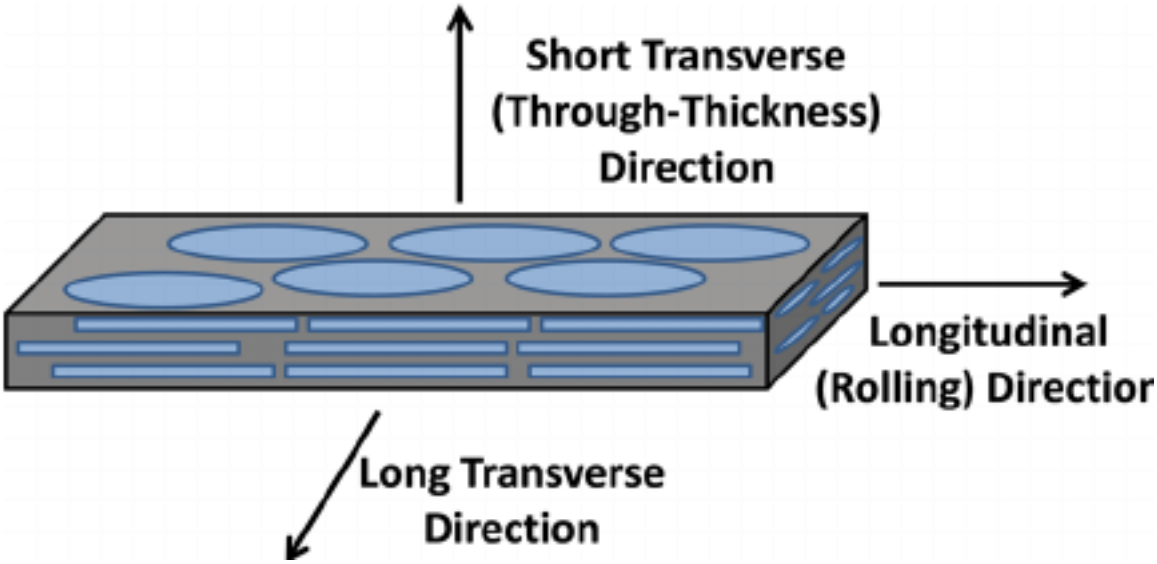

Figure 4.2: Illustration of surface area discrepancy of a rolled defect (37).

4.3 Similarity and Symmetry

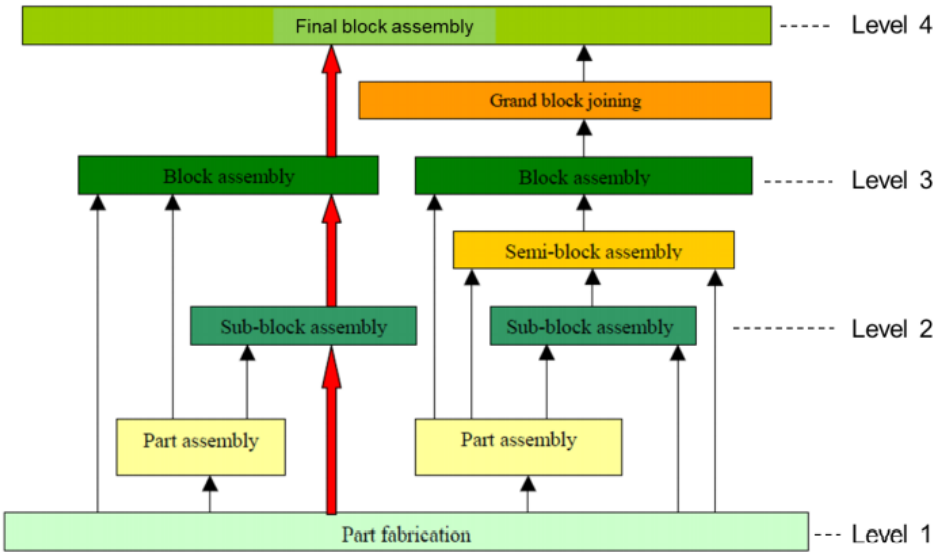

Figure 4.3: Subassembly of similar components.

Similarity and symmetry within an assembly design are beneficial characteristics that improve dimensional accuracy and introduce repetitiveness leading to produc-

tion efficiency. This is achieved by creating symmetry in both geometry and process, which leads to shape stability of the interim parts and support structures that are easily assembled and reconfigured. Without these two aspects, shape stability and proper support, the assembly becomes unpredictable throughout the welding process as shifting, walking, or warping may occur.

In this model, the interim products of the assembly can be thought of as the strips which run the full length of the panel. The strips should be assembled one at a time, working from the center out as to not entrap a buildup of residual stresses.

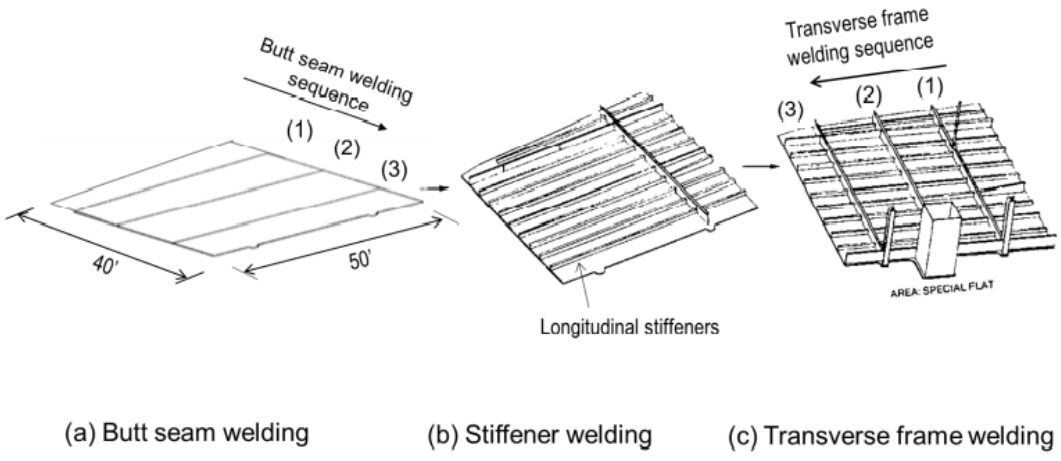

Figure 4.4: Example of proper subassembly and order.

The reduction in plate selection options by taking out the vertical orientation inherently creates more similarity within the design. Additionally, the elimination of the 12 by 5 foot plate from the roulette selection prevents uneven, ill-fitting assembly designs. The decision to add in six by four plates (the largest plate cut in half) allows for more efficient filling of the panel.

As shown above, the similarity and simplicity of these interim components creates a repetitive task that can be completed within one workstation of a manufacturing floor with little to no adjustments. This increases the efficiency of not only the production by minimizing set-up time but also for the laborer who now has a relatively repetitive task to do.

4.4 Plate Robustness

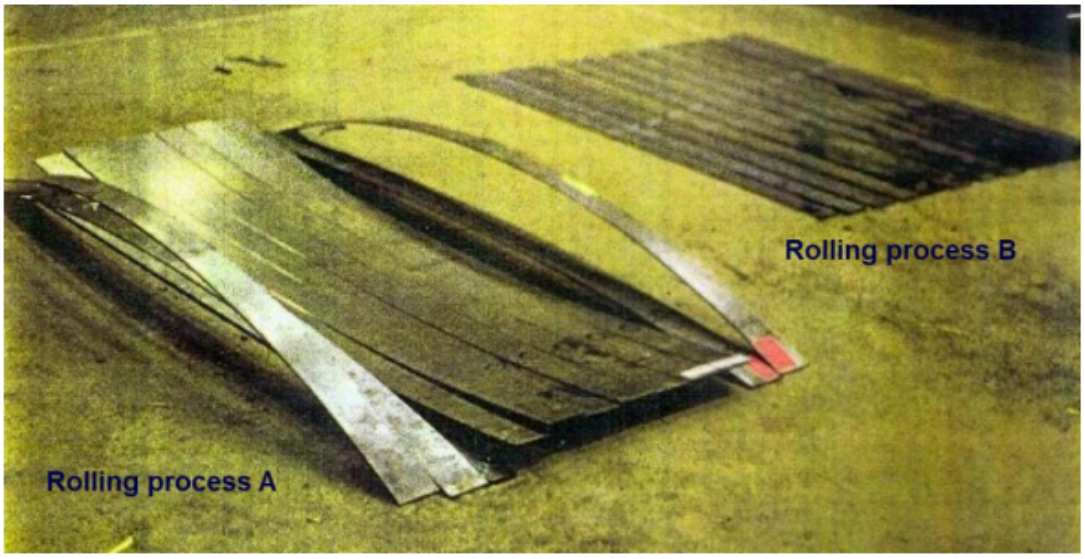

Figure 4.5: Example of effects of material treatment on performance (38).

Robustness of a material or structure is typically described as a resistance to failure when experiencing atypical circumstances outside of expected conditions. Repetition and consistency within the structure or microstructure are crucial to robustness.

Typically this is thought of as construction within a high tolerance of specifications. For example, a plate needs to have a uniform thickness across the length and

width. However, this does not describe the full picture. A plate may be rolled to a specific thickness, but the process to ensure that consistency may have induced significant stresses into the plate [38].

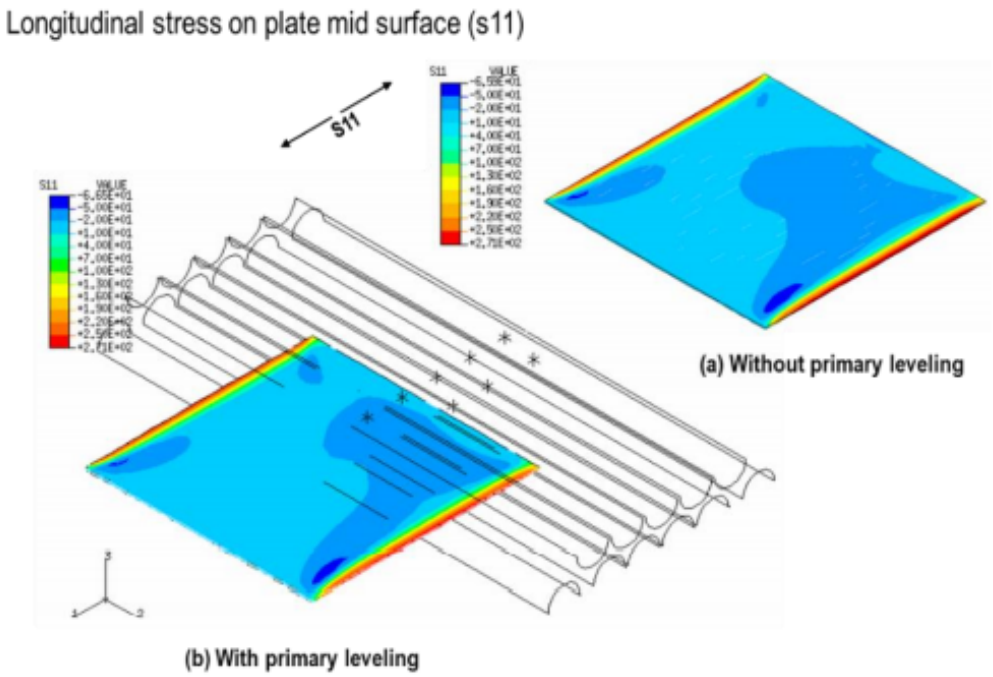

Figure 4.6: Longitudinal stress of a plate mid-surface (38).

Temperature can have a significant impact on grain size of the microstructure [39], as well as the stress distribution across the plate.

Lastly, any post-processing procedures can again effect the specifications, microstructure, and residual stress [40].

Any stresses built up within the plate reach a state of equilibrium. Once these plates are brought into a manufacturing setting, and any procedure, whether it be cutting or welding, disrupts this equilibrium, the plate reacts through 'walking' (the plate shifts through the procedure) or distortion. This typically means the overall

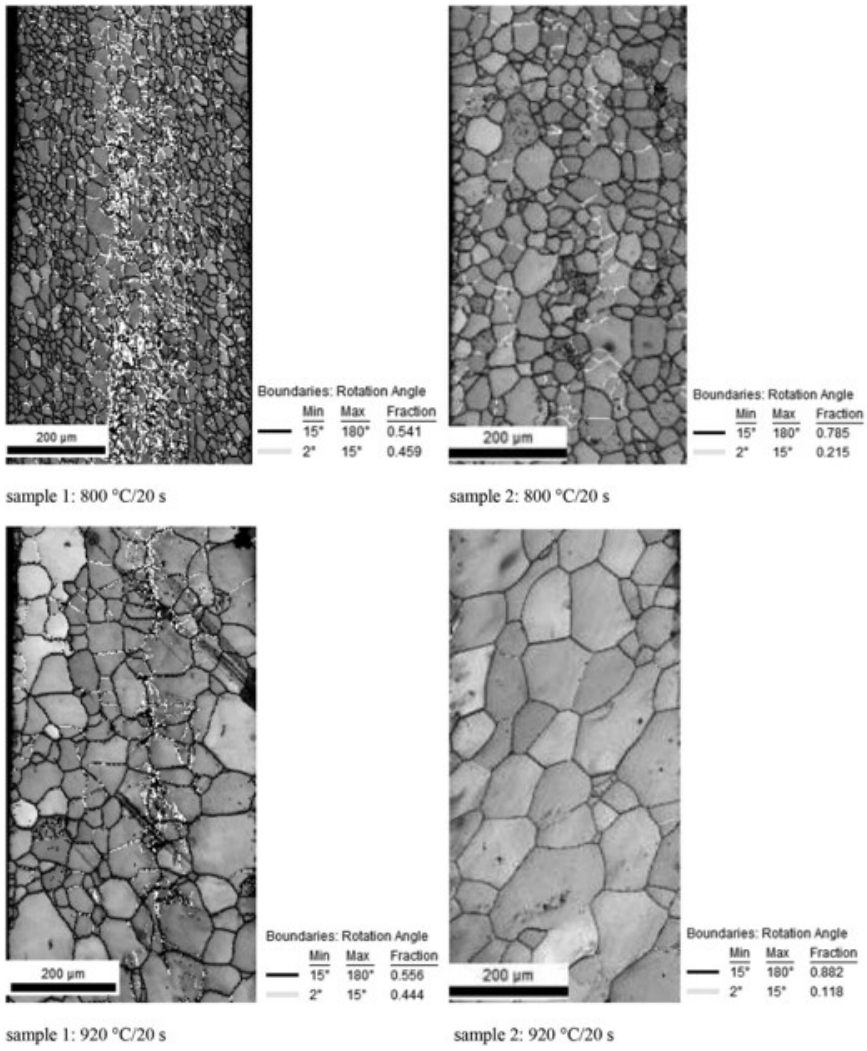

Figure 4.7: Example of effects of annealing temperature on microstructure (39).

structure will no longer meet its set tolerances, and the pieces have to be reworked or even totally scrapped. Should a structure that does not meet tolerances be used, the fitting required may add additional stresses and any misalignment becomes a new stress concentration point.

For all these reasons, plate selection is crucial to a sound structure assembly. However, because ground combat vehicles consist of materials constructed by manufacturers specified by the U.S. Army, there is little adjustment to be made at this time. In the future, a discussion on plate dimensions which produce the most uniform

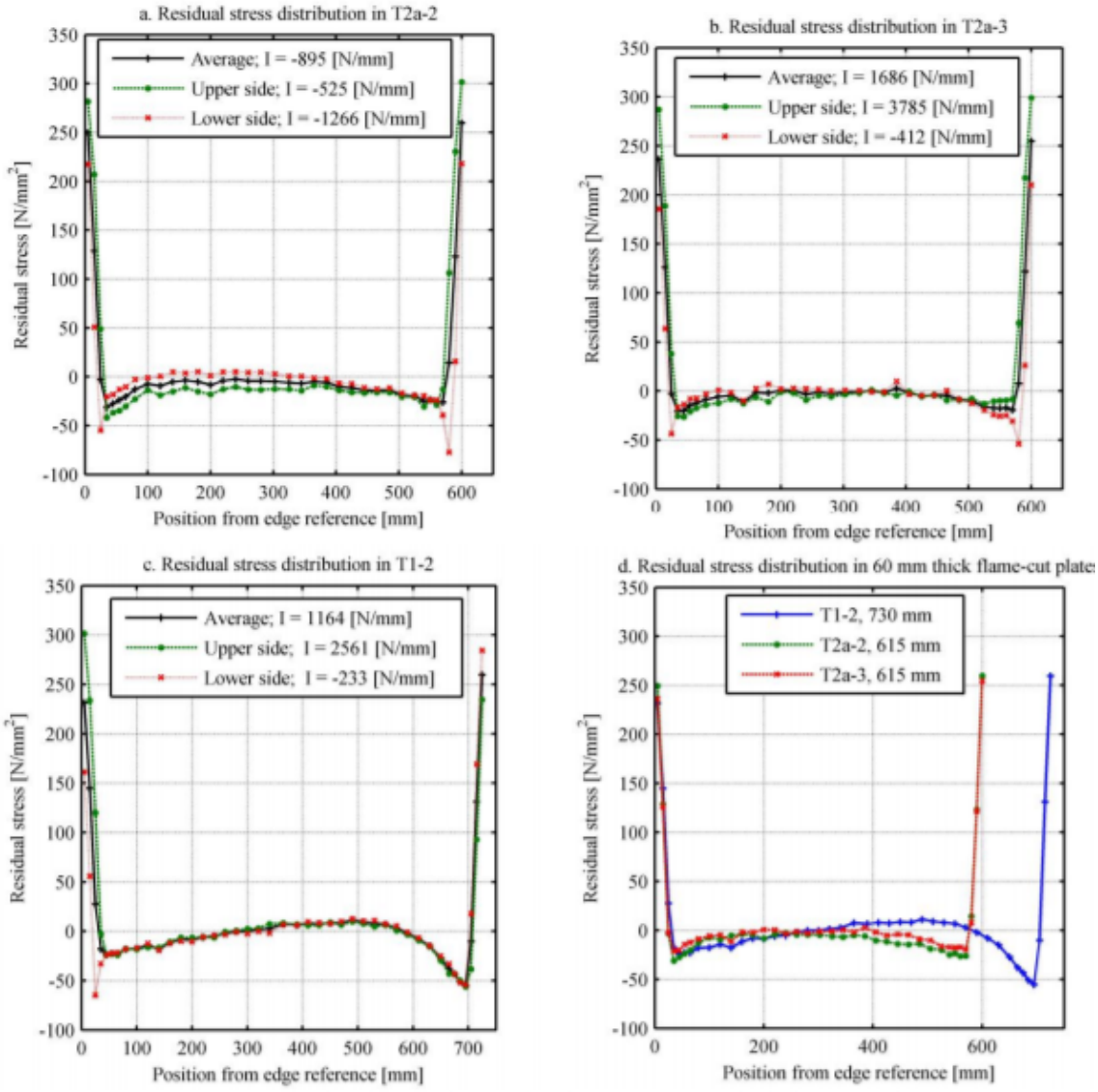

Figure 12: Results of residual stress distribution in 60 mm thick flame-cut plates.

Figure 4.8: Residual stress from flame cutting (40).

characteristics, therefore the most robust plates, should be included when building ground combat vehicles.

CHAPTER V

Final Algorithm

5.1 Introduction

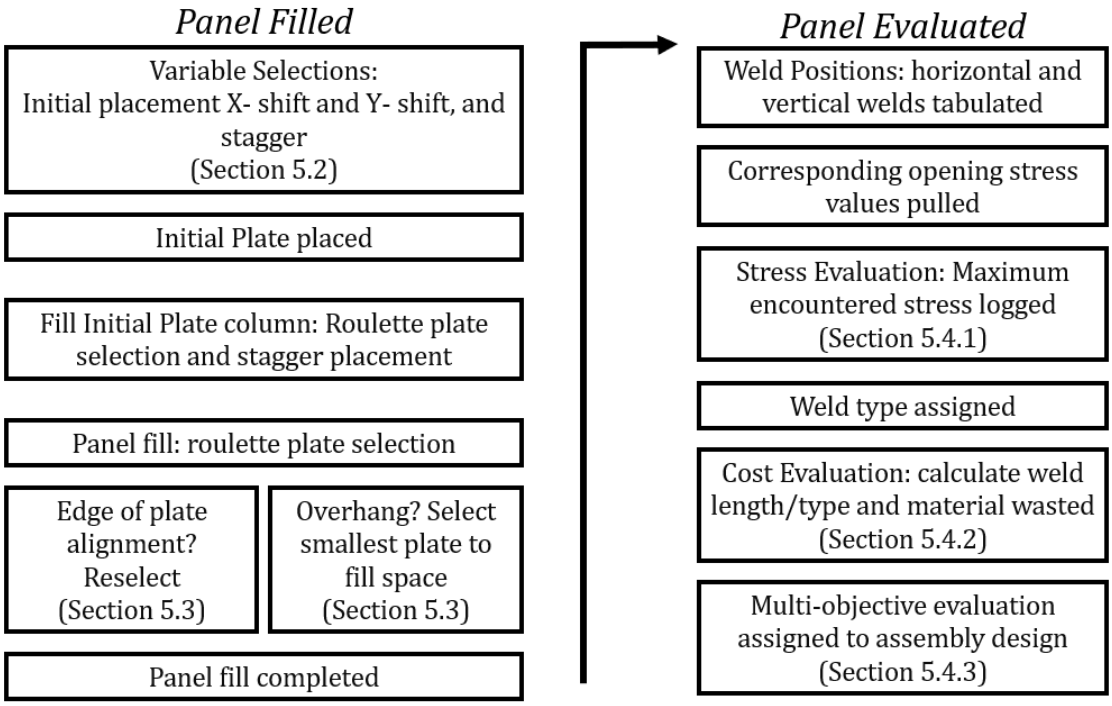

Figure 5.1: Flow Diagram of Algorithm.

The final development stage of the building block algorithm incorporates the manufacturing considerations discussed as well as new constraints and stipulations to un-

burden the optimization from decisions with intuitive or well-defined solutions. This includes covering the highest stress region with a plate, assigning weld type based on a stress-encountered threshold, and using the smallest plate possible in an overhang scenario.

5.2 Initial Placement Variables

Because the primary objective of this optimization is to improve fatigue life by minimizing stress exposure, avoidance of the highest stress region is clearly desirable. Therefore, the decision to start the panel assembly by covering this region provides an intuitive solution for this goal.

The algorithm begins by searching out the highest stress value (S) from the finite element analysis model. Then, values are scanned in all four directions (X1, X2, Y1, Y2) out from this position until a 25 percent drop in stress is detected. These four stress-drop points define a four-sided area, and the centroid of this shape becomes the centroid of the initial placement position.

$$X1 = find(rs, rs + i) <= 0.75 \times max(S) \tag{5.1}$$

$$X2 = find(rs, i - rs) <= 0.75 \times max(S) \tag{5.2}$$

$$Y1 = find(cs, cs + i) <= 0.75 \times max(S) \tag{5.3}$$

$$Y2 = find(cs, i - cs) <= 0.75 \times max(S) \tag{5.4}$$

However, because this algorithm is multi-objective and works in a balance of goals, a stagnant initial position does not allow for a compromise in objectives and restricts

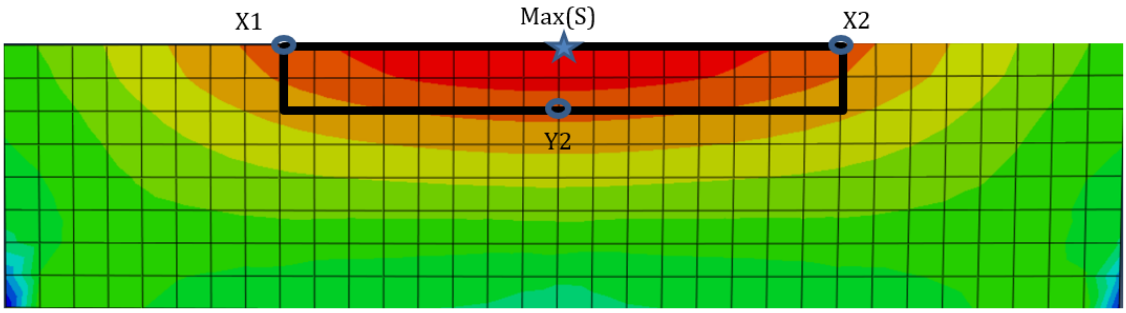

Figure 5.2: Example of initial placement evaluation.

the assembly design pool. Therefore, two new variables are introduced to allow for a shift in the x- and y- directions of the designated centroid.

The largest plate size available always fills the initial position in order to cover as much of the high stress region as possible. The x- and y- shifts should not exceed 50 percent of the initial plate size as to avoid placing the plate edges in the exact location to be avoided, but beyond that, the range allowed for the plate to shift is up to the user. For this case, a 25 percent shift in the length and width of the plate was designated.

The next step fills in the region above and below the initially placed plate, now referred to as the initial column. This is done by the designation of another variable of the algorithm called the stagger. This variable sets the distance to offset the new plates, selected in the roulette wheel, from the initial plate. This stagger selection provides similarity and consistency in the design and aides in preventing a through-width or 'guillotine cut' weld.

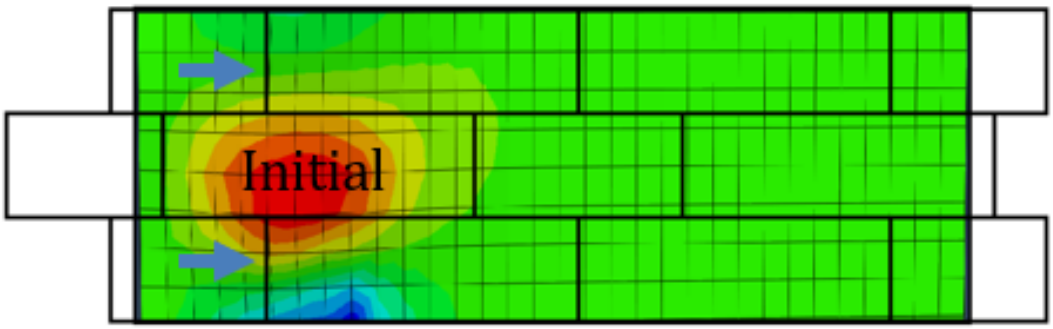

Figure 5.3: Example of stagger condition.

5.3 Constraints

The stagger variable aims to systematically prevent two edges of plates aligning, creating a long, through-width weld. This is not idea as any crack propagation, should it occur, has a significantly longer path to follow instead of being interrupted by a horizontal weld. However, due to the variation of the plate sizes, edge alignment is still possible, and a constraint must be in place to prevent its occurrence.

The constraint simply looks at the edge position of the plate being placed and checks the x-position of previously assigned plates. If the edge of this plate lines up with another, the selection is thrown out, and one of the remaining two options is chosen. The constraint checks the new block edge, and as long as there is no alignment, the plate is positioned.

The previous building block algorithm was designed to allow overhang and overlap. The overlapping scenario primarily allowed for a better fit for vertical and horizontal plates and is no longer relevant to the work. The current development stage is now

designed without overlap capability. Overhang, however, is still necessary as most assemblies do not perfectly fill the panel area.

The algorithm is already checking the far edge of the plate being placed for the alignment constraint; therefore, it can see if a plate is going to overhang the designated area. In an effort to make the optimization more logical and reflective of manufacturing decision-making, the smallest plate that fills the space is now selected. For instance, if the roulette wheel selects a 12-foot plate that overhangs the design space four feet, this constraint kicks in a six-foot plate in its place. This constraint minimizes the material wasted leading to a more viable set of designs.

Vertical Length	Horizontal Length	Roulette Wheel Range
4	6	0-0.333
4	8	0.334-0.666
4	12	0.667-1

Table 5.1: Roulette Wheel ranges for final development stage.

5.4 Evaluations

The algorithm fills in the panel following the new set of variables and constraints. The last step for the optimization is the evaluation of the stress exposure and cost associated with the design decisions.

5.4.1 Stress Evaluation

The weld positions are defined by the borders of the plates placed into the panel assembly. The vertical and horizontal positions are tabulated separately, as the two sets pull from the corresponding x- and y- opening stress values from the finite el-

ement model. Weld type (butt, v, or double-v) is assigned by the maximum stress encountered by each position.

$$for(WeldType)_i$$

$$S(1, X_i) = S(1, X_i) \times SCF_i \tag{5.5}$$

$$S_i = S_i / max(S) \tag{5.6}$$

Then, the maximum stress encountered for the overall panel demarcates the stress exposure evaluation of this design. It should be noted that the average stress encountered over the total length of welds was initially calculated as well. However, the difference in value between designs was so unappreciable between assemblies that the value was dropped as a factor. This could be revisited in other cases with a more complex stress distribution.

5.4.2 Cost Evaluation

The cost of the design depends on the weld length, weld type, and material wasted.

The Navy weld cost model was used to determine cost of each weld type per length. The algorithm simply tallies up the total cost of the welds designated. Since the panel area is consistent between each design, the material wasted provides a more descriptive evaluation. These values are attached to their respective design until the algorithm completes running the designated number of populations.

Once all designs are complete, the algorithm scales these two values by the largest in each category (i.e., the highest cost and most wasted material now have an eval-

uation of '1'). Then, the two values are summed and averaged to provide an overall cost evaluation. While these two factors are currently equally weighted, a preference in consideration for one could easily be adjusted here.

$$TWL_i = TWL_i/max(TWL) \tag{5.7}$$

$$WM_i = WM_i/max(WM) \tag{5.8}$$

$$TC_i = 0.5(TWL_i) + 0.5(WM_i) \tag{5.9}$$

5.4.3 Overall Evaluation

The stress (S) and cost (TC) evaluations for each design then feed into an overall evaluation for the assembly (AE). The two objectives are weighed equally in this study, but these values are easily adjusted to reflect the user or manufacturer's preference. The algorithm concludes with a ranking of the designs by the overall evaluation.

$$AE_i = 0.5(TC_i) + 0.5(S_i); \tag{5.10}$$

5.5 Final Results

The following results represent the highest and lowest, i.e. the best and worst, along with some mid-ranking evaluations from convergent runs of the final building block algorithm.

The first example evaluates a central stress distribution.

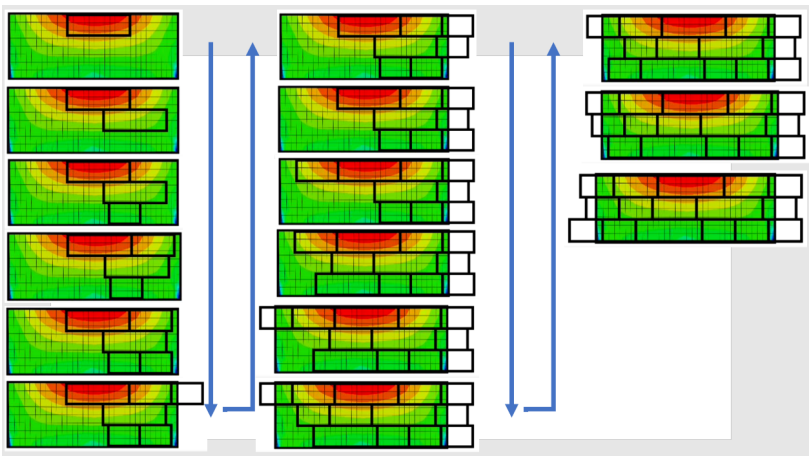

Figure 5.4: Example of a low evaluation panel assembly with a central stress distribution.

The poorly ranked example shown here exhibits a large number of plates used, increasing weld length and material waste. The welds along the initial placement fall within a high stress range, causing a poor stress evaluation as well.

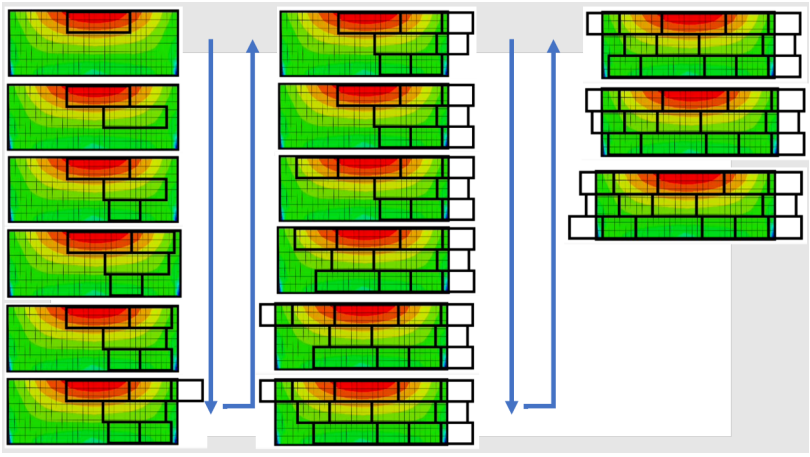

Figure 5.5: Example of a mid-ranking evaluation panel assembly with a central stress distribution.

A mid-ranking assembly has a lower number of plates, but the higher initial placement shift value moves the design into a higher stress region.

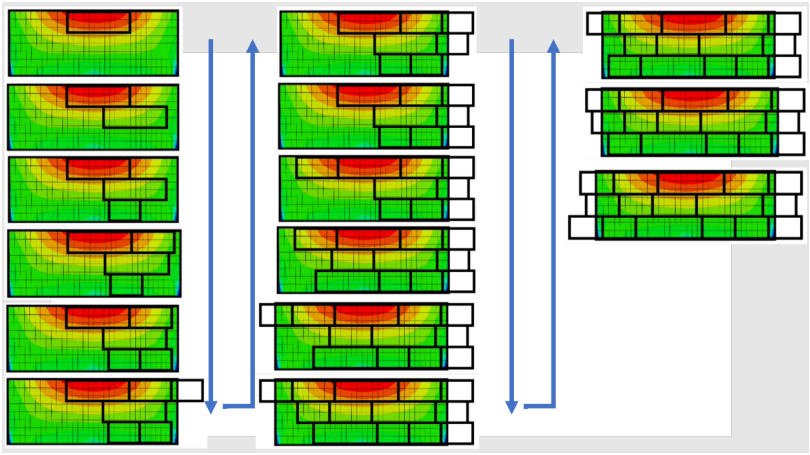

Figure 5.6: Example of a high evaluation panel assembly with a central stress distribution.

The highly ranked evaluation uses a smaller number of plates than the lower ranked assembly plan. The initial placement is moved slightly away from the higher stress region. The overall evaluation is therefore more beneficial in both the cost and stress evaluations.

The next example evaluates an offset stress distribution, showing the efficacy of the initial placement stipulation and algorithm in a variety of scenarios.

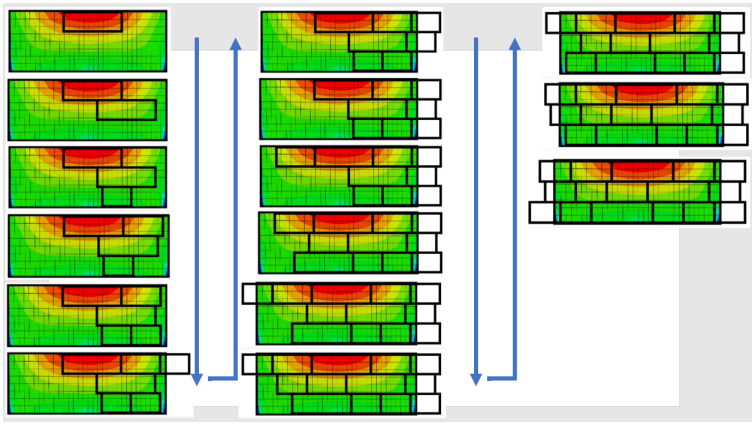

Figure 5.7: Example of a low evaluation panel assembly with a side stress distribution.

The poorly ranked example shown here exhibits similar characteristics as the central stress distribution evaluation: high number of used plates and initial placement fall within a high stress range.

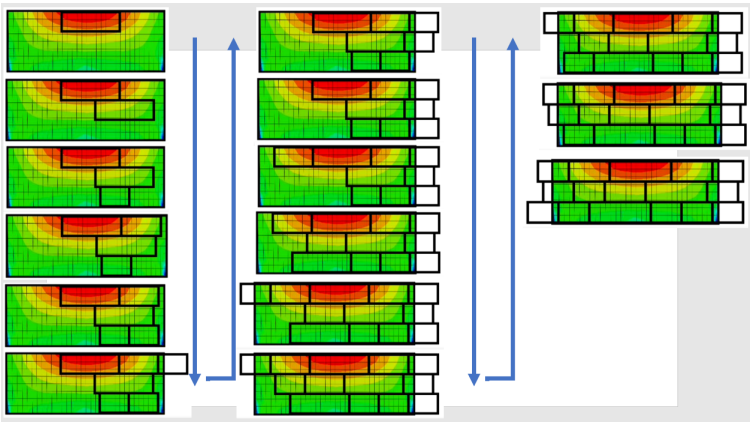

Figure 5.8: Example of a mid-ranking evaluation panel assembly with a side stress distribution.

This mid-ranking assembly has similar characteristics to the central load case: the number of plates decreases, but the stress exposure increases.

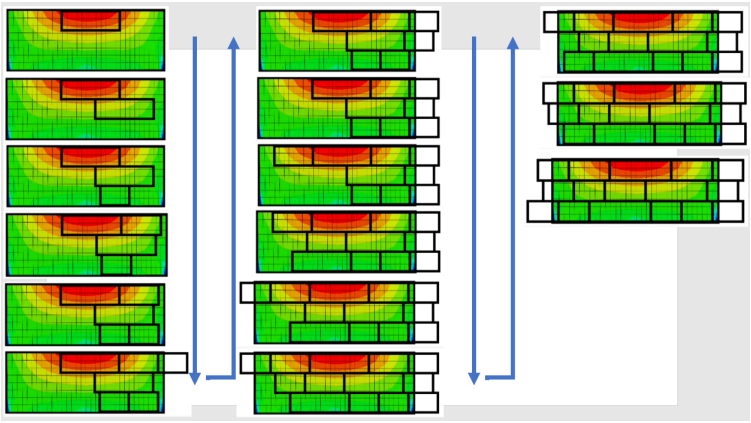

Figure 5.9: Example of a high evaluation panel assembly with a side stress distribution.

The best ranked evaluation in this instance exemplifies the balance of cost and stress. While the initial placement does move through a higher stress region, this

positioning allows for zero material waste. Therefore, this initial sacrifice provides an overall better design.

Overall, the top-ranking designs typically have similar qualities: low number of plates used and low initial shift value. The low number of plates has several implications. The fewer plates used means fewer welds are required, decreasing the cost of the weld, as well as the vulnerability to stress exposure. By using fewer plates the repetition in the design increases as well. The low initial placement shift values means the majority of the high stress region remains covered, decreasing the possibility of significant stress exposure in the design.

Building Block Optimization

Step 1:

Define panel width (W), length (L), and create a matching array of zeros.

Step 2:
Define number of blocks (n) and their lengths and widths in a block index. Set probability of blocks in roulette wheel (for even probability, p = 1/n).

Step 3:
Find most top, left zero position in array, defined by row and column.

Step 4:
Select block from roulette wheel. Place block in designated position.

Step 5:
Index block dimensions and initial position.

Step 6:
Check sum of panel array. Repeat Steps 1-5 until sum equals area (P).

Step 7:
Tabulate vertical and horizontal 'weld' positions from the index of blocks and initial positions.

Step 8:
Trim welds of any overhang (x>W, y>L) and any overlap (preference to earlier placed block). Calculate total weld length.

Step 9:
Calculate area of blocks used and subtract panel area for wasted material.

Step 10:
Read opening stress values for weld positions. Store stress values and maximum stress.

Step 11:
Assign weld type based on stress level threshold and scale stress value by the stress concentration factor.

Step 12:
Repeat Steps 1-11 until desired number of assemblies is created.

Step 13:
Calculate cost evaluations. Scale total weld length and wasted material for each assembly by maximum value, then calculate total cost evaluation.

Step 14:
Calculate total evaluation for each assembly.

Step 15:

Rank all assemblies. Lowest total evaluation is the highest-ranking assembly.

Adding Initial Placement

Step 1:
Find maximum stress value (MV) on panel and define positions of 25% drop. Define centroid of area.

Step 2:
Generate shift and stagger values. Place initial block and follow building block Steps 4 – 15.

Figure 5.10: Building Block Optimization Steps.

CHAPTER VI

Research Summary

6.1 Research Contributions

These optimization algorithms provide an analytical method to developing an assembly plan, moving construction of ground combat vehicles beyond simply following previous procedures.

The initial panel assembly multi-objective algorithm provided a simplistic proof-of-concept, showing that stress exposure and cost could be mutually considered in the design phase of an assembly. The building block optimization brought more manufacturing considerations to the algorithm, representing a more typical build scenario and examining plate selection more closely. The final results produce efficient and effective assembly plans. The high ranking designs typically exhibited similar characteristics, such as a smaller number of plates, low initial shift values, and repetitive use of plates. These characteristics represent what one may intuitively look for in a fundamentally sound manufacturing plan, and this algorithm provides a systematic tool to produce such a design.

The unique methodologies discussed demonstrate assembly plans complementary to both design and manufacturing, capable of minimizing fatigue failure and cost. The

optimizations are constructed to allow the user flexibility, dependent on the priorities for the structure and manufacturing restrictions. The application of this algorithm is far-reaching, only limited to the understanding of the expected loading of the structure and manufacturing limitations.

6.2 Future Research

While this algorithm produces assembly plans with considerations of fatigue life and cost, there is still opportunity to expand the work into another optimization strategy and consider more factors that may play into the life of a structure.

As previously mentioned, due to the random nature of the plate selection within the algorithm, each assembly can have a different number of plates used to complete the panel. In this form, a genetic algorithm (or any other stochastic, non-gradient method) is immaterial. The optimizer does not have a balanced way to compare, let alone produce, these assemblies. Because the computational burden was not significantly detrimental to a Monte Carlo analysis, this method worked well.

However, if a more complex scenario including more factors needed evaluation, an optimization tool that can make strategic decisions for design space evaluation would be very beneficial. This same optimization could be reconfigured into another methodology by including a probabilistic evaluation aspect. In this scenario, the variables such as the initial placement and stagger would remain, and this randomness occurring within the algorithm would be considered by the probabilistic analysis of each run and generation.

Having the capability to search the design space efficiently opens the door to more

variables and considerations. This could include multiple load cases, which could be run as sub-evaluations in a multi-objective algorithm. This would allow the designer to consider multiple scenarios a structure may experience in its life.

6.3 Publication

This work yielded the following publication:

- C. Mayhood, N. Vlahopoulos, "Fatigue-Focused Weld Assembly Optimization", In Proceedings of the Ground Vehicle Systems Engineering and Technology Symposium (GVSETS), NDIA, Nov. 3-5, 2020

BIBLIOGRAPHY

BIBLIOGRAPHY

1. Dong, P. 2005. A Robust Structural Stress Method for Fatigue Analysis of Offshore/Marine Structures. J. Offshore Mech. Arct. Eng., 127 (1), 68-74.

2. American Welding Society, 2004. Welding Handbook Volume 1: Welding Science Technology.

3. U.S. Army, 2006. SPC 12479550, Ground Combat Vehicle Welding Code - Steel. Revision A.

4. Dong, P., Zhou, W., Xing, S. (2019). An Analytical Method for Interpreting Distortion Effects on Fatigue Test Results of Thin Plate Panel Specimens. Welding in the World, 63 (6), 1707-1714.

5. Xing, S., Dong, P. (2016). An Analytical SCF Solution Method for Joint Misalignments and Application in Fatigue Test Data Interpetation. Marine Structures, 50 (1), 143-161.

6. Dong, P. (2005). Residual Stresses and Distortions in Welded Structures: a Perspective for Engineering Applications. Science and Technology of Welding and Joining, 10 (4), 389-398.

7. U.S. Army, 2020. Regulation 750–59, Corrosion Prevention and Control for Army Materiel.

8. U.S. Army, 1984. TOP 2-2-710, Ballistic Tests of Armor Materials.

9. Optistruct 2019.1, Altair.

10. Mi, C., Wentai, L., Xuewen, X., Haigen, J., Zhengqi, G., Filippo, B. 2019. Lifetime Assessment and Optimization of a Welded A-Type Frame in a Mining Truck Considering Uncertainties of Material Properties and Structural Geometry and Load. Applied Sciences 9, Nr. 5: 918.

11. Gao, Y., Wenzhong, Z. 2014. Adaptive Optimization with Weld Fatigue Constraints Based on Surrogate Model for Railway Vehicles. Mechanics Based Design of Structures and Machines 42, Nr. 2: 244-254.

12. Takeda, N., Naruse, T., Tomohrio, N. 2013. Can we Optimally Design Light-Weight Welded Structures with Sufficient Fatigue Resistance?. 10th World Congress

on Structural and Multidisciplinary Optimization.

13. Liu, Y., Yin, Y., Lu, Y. 2011. Multi-Objective Optimization of a Bolt-Flange Structure. Advanced Materials Research 233-235: 2800-2804.

14. Vasu, A., Xing, S., Mei, J., Chung, C.J., Ravi, D. 2018. A Computational Methodology for Multi-Objective Fatigue Life Optimization of Welded Brake Flange on Full Beam Axles. SAE Technical Paper 2018-01-1019.

15. Callens, A., André, B. 2012. Fatigue Design of Welded Bicycle Frames using a Multiaxial Criterion. Procedia Engineering 34: 640-645.

16. Masatoshi, S., Yang, L., Kousaku, I. 2020. Optimum shape design of thin-walled cross sections using a parameter-free optimization method. Thin-Walled Structures 148: 106603.

17. Norio, T., Tomohiro, N. 2014. Optimal design of welded structure with structural and local-notch stresses based on International Institute of Welding recommendations. Structural and Multidisciplinary Optimization 51, Nr. 5: 1133-1147.

18. Kirthana, S., M.K. Nizamuddin. 2011. FEA and Topology Optimization of an Engine Mounting Bracket. International Journal of Current Engineering and Technology.

19. Zhao, X., Li, F., Liu, Y., Fan, Y. 2015. Fatigue Behavior of a Box-Type Welded Structure of Hydraulic Support Used in Coal Mine. Materials 8, Nr. 10: 6609-6622.

20. Liao, Y. 2003. A Genetic Algorithm-based Fixture Locating Positions and Clamping Schemes Optimization. Proceedings of the Institution of Mechanical Engineers, Part B: Journal of Engineering Manufacture 217, Nr. 8: 1075-1083.

21. Cai, W. 2008. Fixture Optimization for Sheet Panel Assembly considering Welding Gun Variations. Proceedings of the Institution of Mechanical Engineers, Part C: Journal of Mechanical Engineering Science 222, Nr. 2: 235-246.

22. Bhatti, Q., Ouisse, M., Cogan, S. 2011. An Adaptive Optimization Procedure for Spot-Welded Structures. Computers Structures 89, Nr. 17-18: 1697-1711.

23. Liao, Y. 2004. Optimal Design of Weld Pattern in Sheet Metal Assembly based on a Genetic Algorithm. The International Journal of Advanced Manufacturing Technology 26, Nr. 5-6: 512-516.

24. Dong, P. 2001. A Structural Stress Definition and Numerical Implementation for Fatigue Analysis of Welded Joints. International Journal of Fatigue 23, Nr. 10:

865-876.

25. Dong, P., Prager, M., Osage, D. (2007). The Design Master S-N Curve in ASME Div 2 Rewrite and its Validations. Welding in the World, 51 (5), 53-63.

26. Dong, P., Hong, J.K., Osage, D., Dewees, D., Prager, M. (2010). The Master S-N Curve Method and Implementation for Fatigue Evaluation of Welded Components in the ASME BPV Code, Section VIII, Div 2 and API 579-1/ASME FFS-1 no. 523.

27. Abaqus/CAE 2019, Simulia.

28. Hobbacher, A. 2015. Recommendations for Fatigue Design of Welded Joints and Components. Springer International Publishing.

29. U.S. Navy, 2019. Steelworker Advanced, NAVEDTRA 14251A. Welding Costs.

30. Matlab, version 9.6 (R2019a), Mathworks Inc.

31. Liu, D., Tan, K., Huang, S., Goh, C., Ho, W. 2008. On Solving Multiobjective Bin Packing Problems using Evolutionary Particle Swarm Optimization. European Journal of Operational Research 190, Nr. 2: 357-382.

32. Dighe, R., Jakiela, M. 1995. Solving Pattern Nesting Problems with Genetic Algorithms Employing Task Decomposition and Contact Detection. Evolutionary Computation 3, Nr. 3: 239-266.

33. Burke, E., Kendall, G., Whitwell, G. 2004. A New Placement Heuristic for the Orthogonal Stock-Cutting Problem. Operations Research 52, Nr. 4: 655-671.

34. Da Silva, R., Parpinelli, R. 2017. Playing the Original Game Boy Tetris Using a Real Coded Genetic Algorithm. Brazilian Conference on Intelligent Systems.

35. Langenhoven, L. 2010. Swarm Tetris: Applying Particle Swarm Optimization to Tetris. Institute of Electrical and Electronics Engineers.

36. Sarkar, P. 2020. Analysis of Failure of a Chassis Long Member Manufactured from E-46Grade Hot-Rolled Steel Coil. Journal of Failure Analysis and Prevention 20, 819–832.

37. Whelchel, R., Kennedy, G., Dwivedi, S., Sanders, T., Thadhani, N. 2013. Spall Behavior of Rolled Aluminum 5083-H116 Plate. Journal of Applied Physics 113.

38. Huang, T., Dong, P., DeCan, L. (2004). Fabrication and Engineering Technology for Lightweight Ship Structures, Part 1: Distortions and Residual Stresses in Panel Fabrication, 20 (1), 43-59.

39. Schneider, J., Stöcker, A., Franke, A., Kawalla, R. 2018. Effects by the Microstructure after Hot and Cold Rolling on the Texture and Grain Size after Final Annealing of Ferritic Non-Oriented FeSi Steel. AIP Advances 8.4.

40. Thiébaud, R., Lebet, J. 2012. Experimental Study of Residual Stresses in Thick Steel Plates. Proceedings of the Annual Stability Conference Structural Stability Research Council.